

Summary and Outlook

4th International Fermi Symposium

Seth Digel, KIPAC/SLAC, 2 November 2012

Thanks

Local Organizing Committee

Tom Langenslein - chair, Stanford University, USA
Nancy Christiansen, Stanford University, USA
Lynn Cominsky, Sonoma State University, USA
Jan Goebel, Stanford University, USA
WenLi Heffner (a.k.a Lucy Zhou), Stanford University, USA
Peter Michelson, Stanford University, USA
Nicola Dmodel, Stanford University, USA
Steve Ritz, University of California Santa Cruz, USA
Giovanna Benatore, Stanford University, USA

+ Bob Kahn
+ Dorrene Ross



International Science Organizing Committee (SOC)

William Atwood (UCSC)
Ronaldo Bellazzini (INFN, Pisa)
Roger Standford (Stanford/KIPAC)
Elliott Bloom (SLAC/KIPAC)
James Buckley (WashU)
Fernando Camilo (Columbia U and Arecibo)
Patrizia Caraveo (INFN-UIAF, Milano)
Eric Charles (SLAC)
Charles Dermer (NRL)
Seth Digel (SLAC/KIPAC)
Dale Frail (NSF)
Bryan Gaensler (U Sydney)
Neil Gehrels (GSFC)
Jochen Greiner (MPE)
Isabelle Grenier (Laboratoire AIM, Saclay)
Elizabeth Hays (GSFC)
Dairde Horan (LLR)
Buell Jannuzi (U of Arizona)
Victoria Kaspi (McGill U)
Nobuyuki Kawai (Tokyo)
Luca Latronico (INFN Torino)
Alan Marscher (BU)
Peter Michelson (Stanford)
Jonathan Ormes (Denver)
William Paciosas (UA Huntsville)
Anthony Readhead (Caltech)
Steven Ritz (UCSC)
Andrew Strong (MPE Garching)
Gino Tosti (INFN and University Perugia)
Stefan Wagner (Heidelberg)
Colleen Wilson-Hodge (MSFC)

- To NASA, DOE, & international agencies for supporting the mission
- To all conference contributors (& session chairs!)

Julie McEnery & Terri Brandt

Patrick Lee Nolan (1952-2011)



Title: Gamma large area silicon telescope: Applying SI strip detector technology to the detection of gamma rays in space

Authors: [Arwood, W. B.](#); [Bloom, E. D.](#); [Godfrey, G. L.](#); [Hertz, P. L.](#); [Lin, Ying-Chi](#); [Nolan, P. L.](#); [Snyder, A. E.](#); [Taylor, R. E.](#); [Wood, K. S.](#); [Michelson, P. E.](#)

Affiliation: AA(Naval Research Lab., Washington, DC.), AB(Naval Research Lab., Washington, DC.), AC(Naval Research Lab., Washington, DC.), AD(Naval Research Lab., Washington, DC.), AE(Stanford Univ., CA.), AF(Stanford Univ., CA.), AG(Stanford Univ., CA.), AH(Naval Research Lab., Washington, DC.), AI(Naval Research Lab., Washington, DC.), AJ(Stanford Univ., CA.)

Publication: In ESA, Proceedings of an ESA Symposium on Photon Detectors for Space Instrumentation p 227-232 (SEE N04-15025 03-19)

Publication Date: 12/1992

Outline

- State of *Fermi*
- State of *Fermi* Science
 - Subjective Symposium Summary
- Outlook

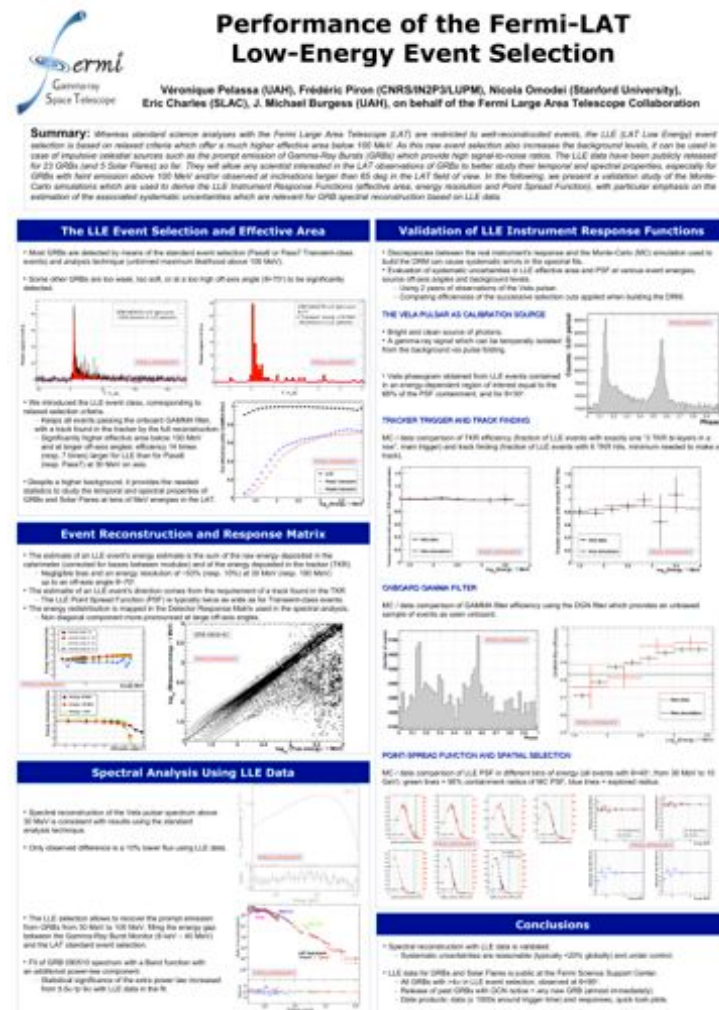
State of *Fermi* – in space

- Julie McEnery: “instruments and spacecraft operate as designed, no degradation in science performance since launch”
- LAT: ~275B triggers, 225M Source class events
- GBM: >1000 GRBs

State of *Fermi* – on the ground

- Analysis and operations updates
 - LAT: LAT Low Energy selection, Pass 7 reprocessing, Pass 8 details (later)
 - GBM: Continuous Time Tagged Event data will be taken starting in November

* N.B. Throughout I have listed only the first named author



Pelassa*

State of *Fermi* – on the ground

- 2012 NASA Senior Review

Panel recommended “funding at the desired level of augmentation to provide for full operations through FY14. We recommend an extension through 2016 with a review in 2014.”

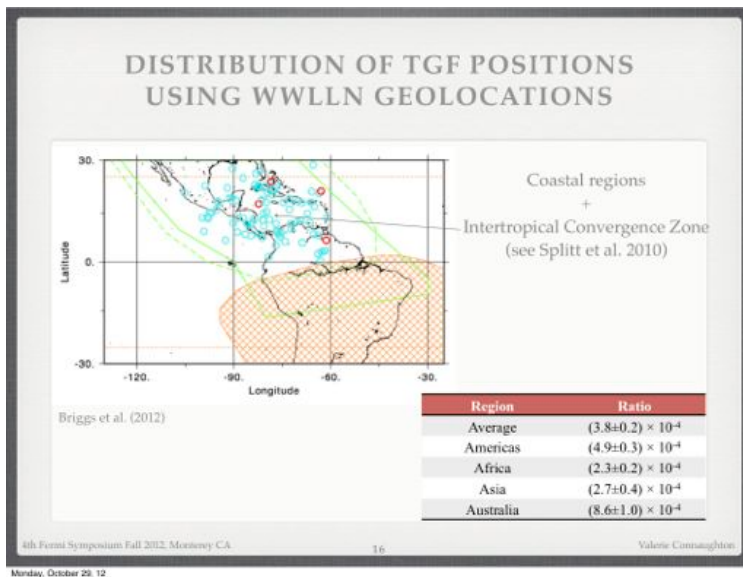
- DOE HEP Cosmic Frontier Review (LAT operations)

“The Fermi team acquitted itself well.” – Roger B.

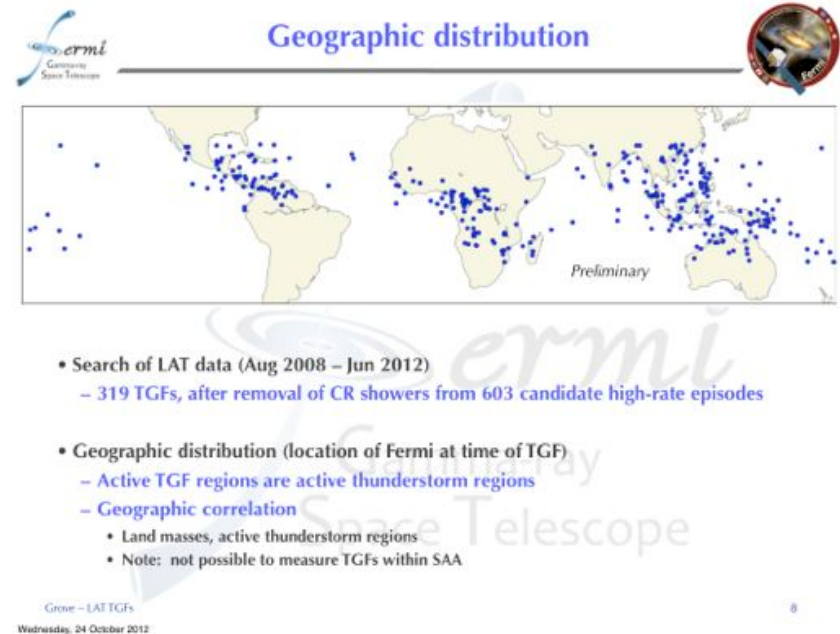
SOLAR SYSTEM

Terrestrial Gama-ray Flashes

- GBM observations and analysis with ground radio arrays



Connaughton

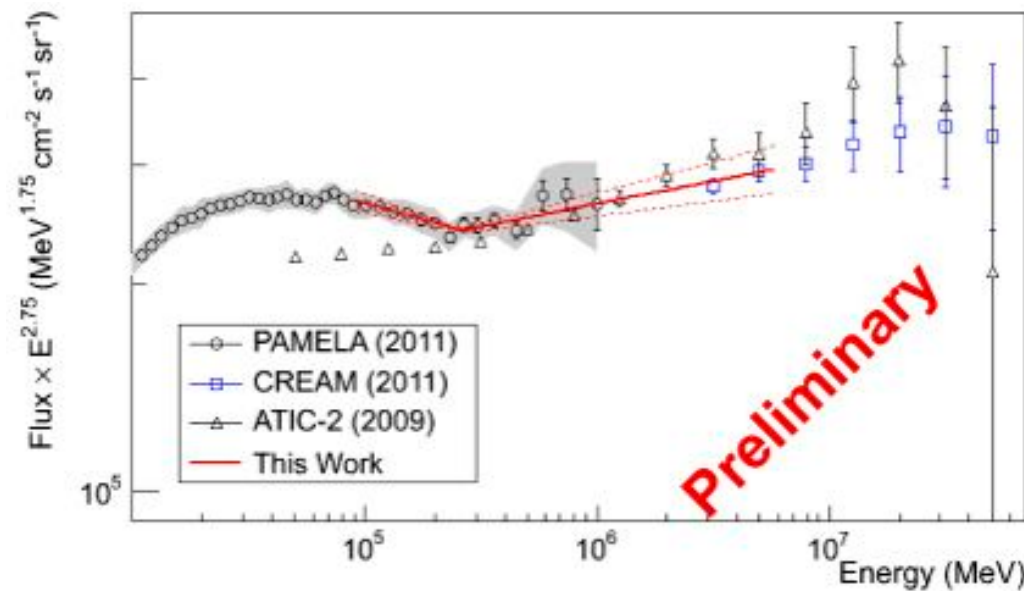


Grove

- LAT detections now also accumulating from carefully timed nadir observations
- Multiwavelength & rich science has continued to develop since 3rd Fermi Symposium

Cosmic-Ray Interactions in the Upper Atmosphere

- Inferring the spectrum of CR protons
 - Indications are that it is consistent with the high-energy break reported by PAMELA



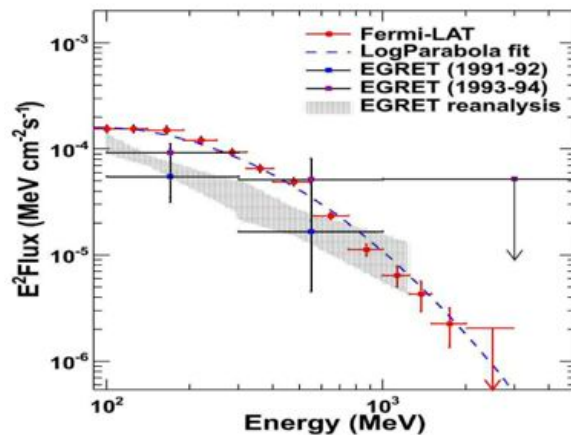
Mithumisiri et al.

The Moon

- A passive gamma-ray source – monitoring the CR flux outside the Earth's magnetosphere



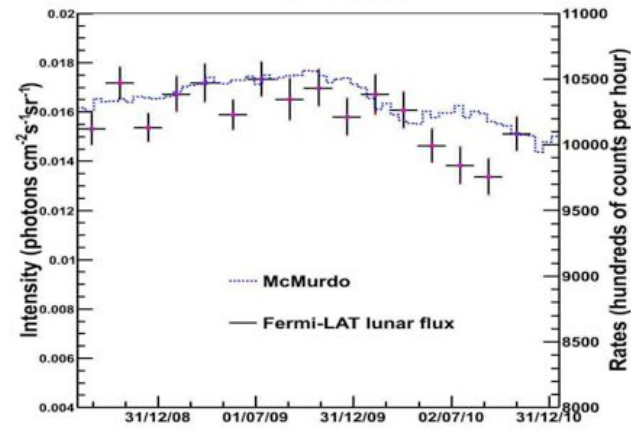
Lunar spectrum (3years) from the paper
(ApJ, 758, 140 2012)



N. Giglietto - IV Fermi symposium 2012



Neutron monitor rates and Lunar emission



N. Giglietto - IV Fermi symposium 2012

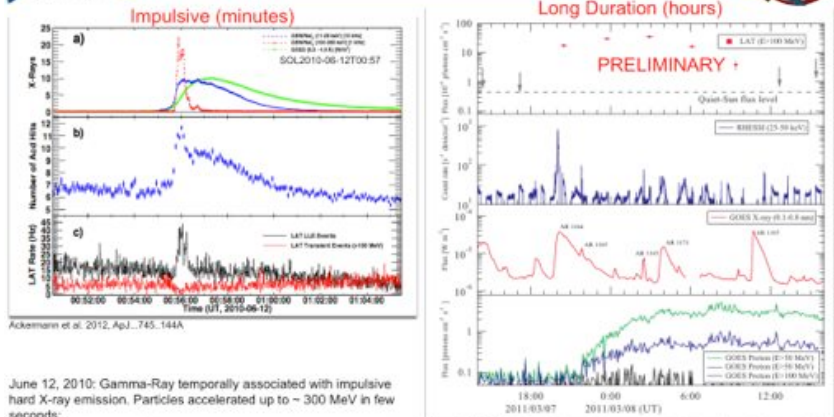
NM data from <http://neutronm.bartol.udel.edu/>

Giglietto

The Sun

- Focus was the transient Sun – the Sun has helped a lot since the 3rd Fermi Symposium

Impulsive vs Long Duration flares >100 MeV



June 12, 2010: Gamma-Ray temporally associated with impulsive hard X-ray emission. Particles accelerated up to ~ 300 MeV in few seconds;
 Hard X-ray pile up in ACD causes suppression of the standard LAT event rate (on-ground classification of gamma-rays)
 Signal recovered in LAT Low Energy Events (looser selection cut)
 Sustained gamma-ray emission not observed

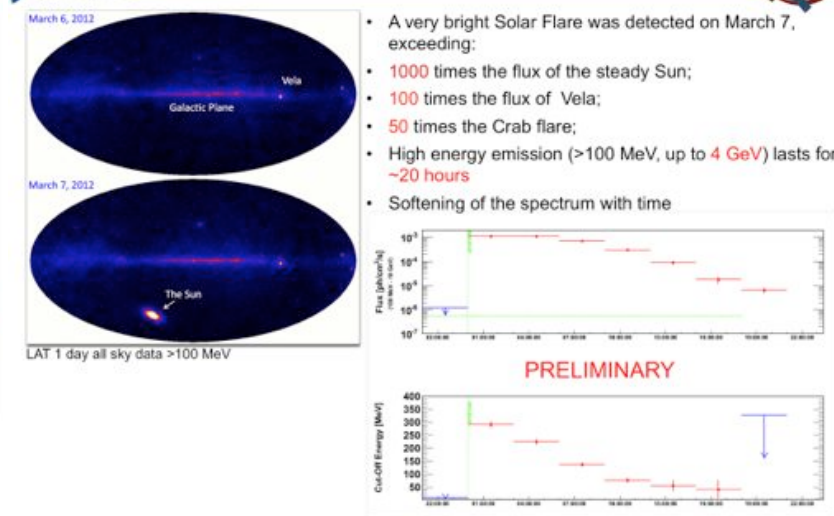
6 Impulsive solar flares to date

March 7/8 2011: Sustained emission associated to one impulsive episode in X-rays;
 Accompanied by modest SEP, but very fast (~2000 km/s) CME;
 Continuous interaction of particles with the Sun for hours after the impulsive flare;

~13 long lasting emission (high significance)

Nicola Omodei – Stanford/KIPAC

The longest lasting gamma-ray emission: March 7, 2012



- A very bright Solar Flare was detected on March 7, exceeding:
 - 1000 times the flux of the steady Sun;
 - 100 times the flux of Vela;
 - 50 times the Crab flare;
- High energy emission (>100 MeV, up to 4 GeV) lasts for ~20 hours
- Softening of the spectrum with time

Nicola Omodei – Stanford/KIPAC

Omodei

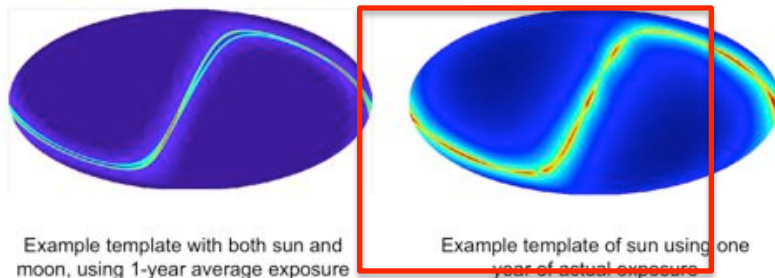
Sun as a Background

- Inverse Compton scattering on the solar radiation field
- Ferrara:



Development for 5-year catalog

- Both quiescent Sun and Moon can be seen in the 4-year integrated data set
 - Developing tools to calculate exposure-corrected templates using measured spectra
 - Sun and Moon templates will be included as an all-sky source in 5-year catalog analysis



22

Solar and stellar inverse Compton emission: a software package
 Elena Orlando (Stanford University/SLAC) and Andrew Strong (MIT)

Software to compute inverse-Compton scattering emission from the heliosphere and the photosphere of stars

ABSTRACT
 We present our software to compute inverse-Compton scattering from the heliosphere, as well as the photospheres of stars. It includes a formalism of radiation in the heliosphere, but it can be used for any user-defined radiation model. It outputs profiles, spectra and differential flux to FITS files in a variety of forms for convenient use. The software is publicly available and it is under continuing development, taking into account updated observations in gamma-ray and cosmic rays. It uses general-purpose inverse-Compton routines with other features like energy loss rates and emissivity for any user-defined target photon and target spectra.

KEYWORDS
 Inverse-Compton scattering, heliosphere, photosphere, gamma-ray emission, cosmic rays, FITS files, differential flux, energy loss rates, emissivity, target photon, target spectra.

KEY DETECTION OF THE SUN IN GAMMA-RAY OBSERVATIONS
 The Sun is a bright source of gamma-ray emission. It is the only source of gamma-ray emission that is visible to the Fermi-LAT. The Sun is a complex system, and its emission is highly variable. The Sun is a source of gamma-ray emission that is visible to the Fermi-LAT. The Sun is a complex system, and its emission is highly variable. The Sun is a source of gamma-ray emission that is visible to the Fermi-LAT. The Sun is a complex system, and its emission is highly variable.

THE SOFTWARE PACKAGE
 The software package is designed to be easy to use and to provide accurate results. It is written in Python and uses the NumPy and SciPy libraries. The software is available on GitHub and can be installed using pip. The software is designed to be easy to use and to provide accurate results. It is written in Python and uses the NumPy and SciPy libraries. The software is available on GitHub and can be installed using pip.

CONCLUSIONS AND FUTURE WORK
 The software package is a valuable tool for studying the Sun and other stars. It is designed to be easy to use and to provide accurate results. It is written in Python and uses the NumPy and SciPy libraries. The software is available on GitHub and can be installed using pip.

ACKNOWLEDGMENTS
 We thank the Fermi-LAT team for providing the data used in this work. We also thank the anonymous referee for their comments and suggestions.

REFERENCES
 Orlando, E., & Strong, A. (2018). Solar and stellar inverse Compton emission: a software package. *Journal of High Energy Astrophysics*, 11(1), 1-10.

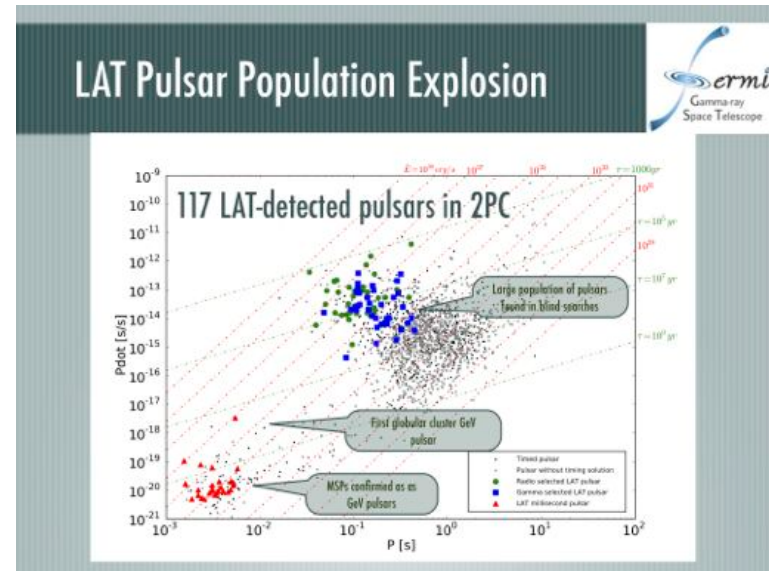
CONTACT
 Elena Orlando: orlando@stanford.edu
 Andrew Strong: astrong@mit.edu

Orlando & Strong

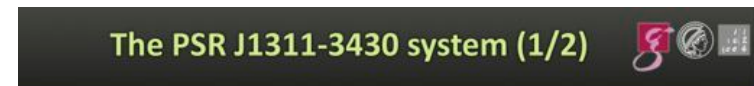
The Galaxy

Pulsars

- Number is still increasing rapidly – projecting >200 soon
 - Increase since 3rd FS has been on all fronts: radio monitoring & follow-up* and blind searches, with spectacular MSP increase
- **First blind search MSP** announced this week: Pletsch et al. found PSR J1311-3430
 - Optical observations (Romani 2012) constrained the search *somewhat*
 - Most compact MSP known & $M_{\text{pulsar}} > 2.1 M_{\text{sun}}$ (Romani et al.)



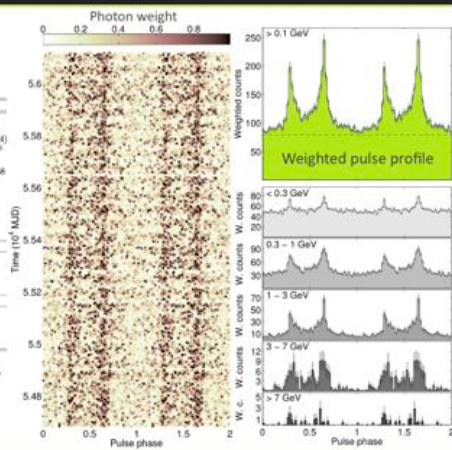
Ray



• Following the discovery: pulsar timing to precisely measure the system parameters (—)

Parameter	Value
Right ascension (J2000.0) (hh:mm:ss)	13:11:45.7242(2)
Declination (J2000.0) (dd:mm:ss)	-34:30:30.355(4)
Spin frequency, f (Hz)	390.5628326407(4)
Frequency derivative, \dot{f} (Hz s ⁻¹)	-3.198(2) × 10 ⁻¹⁹
Reference time scale	TDB
Reference time (MJD)	55266.9078675858
Orbital period P_{orb} (d)	0.0651157335(7)
Projected pulsar semi-major axis a (h-a)	0.010581(4)
Time of ascending node T_{asc} (MJD)	56009.129454(7)
Eccentricity e	< 0.002
Data span (MJD)	54682 - 56119
Weighted RMS residual (μ s)	17
Inferred Quantities	
Companion mass m_2 (M_{sun})	> 0.0082
Spin-down luminosity \dot{E} (erg s ⁻¹)	4.9 × 10 ³⁴
Characteristic age τ_c (yr)	1.9 × 10 ⁶
Surface magnetic field B_s (G)	2.3 × 10 ⁸
Gamma-Ray Spectral Parameters	
Photon index, Γ	1.8 ± 0.1
Cutoff energy, E_c (GeV)	3.2 ± 0.4
Photon flux above 0.1 GeV, F (10 ⁻⁸ photons cm ⁻² s ⁻¹)	9.2 ± 0.5
Energy flux above 0.1 GeV, G (10 ⁻¹¹ erg cm ⁻² s ⁻¹)	6.2 ± 0.2

- No significant evidence for eccentricity.
- Marginal evidence for proper motion.
- No evidence for gamma-ray flux modulation at orbital period.



Pletsch

Pulsars at VHE

- Since the 3rd Fermi Symposium, **VERITAS** studies of the Crab pulsar at >120 GeV have advanced from discovery: Search for correlation with radio giant pulses, limits (with LAT) on Lorentz Invariance Violation
- **MAGIC** reported a stereo measurement of the light curve down to ~50 GeV (and reported the nebula IC peak as 59 ± 6 GeV and the nebula as steady > 300 GeV

KICP VERITAS Observations of the Crab Pulsar
A. MCCANN FOR THE VERITAS COLLABORATION
The University of Chicago, The Kavli Institute for Cosmological Physics,
933 East 58th Street, Chicago, IL 60637 (mccann@kicp.uchicago.edu)

ABSTRACT

The Crab pulsar has been observed over 100 years. These observations have advanced our understanding of pulsars, including their emission mechanisms, their structure, and their energy distribution. A significant discovery was the detection of a giant pulse in 2009, which was recently followed by a second giant pulse in 2012. This paper reports on the search for a third giant pulse during VERITAS observations. We also present some preliminary results on Lorentz invariance violation (LIV) searches using VERITAS data on the Crab pulsar.

Giant Radio Pulses and VHE emission in the Crab pulsar
Introduction: Searching for a VHE-GRP correlation

The Crab pulsar is the only known pulsar whose period increases over time. It is also one of only two pulsars known to emit giant pulses (GPs). GPs have the following characteristics:

- They appear in the same phase range as normal pulses.
- They exhibit an unusual width of magnitude greater than the normal signal.
- They are detected in a wide range of energies from radio to VHE.
- They are detected in a wide range of energies from radio to VHE.

Figure 1: A plot showing the correlation between the Crab pulsar's VHE emission and its radio giant pulses. The x-axis represents the phase range (0 to 1) and the y-axis represents the flux density. The plot shows a clear correlation between the two, with a peak in the VHE emission corresponding to the phase range of the radio giant pulses.

Search Strategy and Monte Carlo

Using the VERITAS and CRAB data, we have conducted a search for a correlation between the Crab pulsar's VHE emission and its radio giant pulses. We used a Monte Carlo simulation to generate a distribution of VHE emission for a given phase range. The results of this search are shown in Figure 2.

Figure 2: A plot showing the results of the Monte Carlo simulation. The x-axis represents the phase range (0 to 1) and the y-axis represents the flux density. The plot shows a distribution of VHE emission for a given phase range, with a peak in the VHE emission corresponding to the phase range of the radio giant pulses.

Search Results and Limits

We have conducted a search for a correlation between the Crab pulsar's VHE emission and its radio giant pulses. The results of this search are shown in Figure 3.

Figure 3: A plot showing the results of the search. The x-axis represents the phase range (0 to 1) and the y-axis represents the flux density. The plot shows a distribution of VHE emission for a given phase range, with a peak in the VHE emission corresponding to the phase range of the radio giant pulses.

Searching for Lorentz Invariance Violation
Introduction: What is Lorentz Invariance Violation?

Lorentz invariance is a fundamental principle of special relativity. It states that the laws of physics are the same for all observers in uniform motion relative to one another. Lorentz invariance violation (LIV) is a hypothetical phenomenon that would violate this principle. There are several different models of LIV, each with its own characteristic energy dependence. We have searched for LIV using VERITAS data on the Crab pulsar.

Figure 4: A plot showing the results of the LIV search. The x-axis represents the energy (GeV) and the y-axis represents the LIV parameter. The plot shows a distribution of LIV parameters for a given energy range, with a peak in the LIV parameter corresponding to the energy range of the Crab pulsar.

Using the Crab pulsar seen by Fermi and VERITAS

Figure 5: A plot showing the Crab pulsar's emission as seen by Fermi and VERITAS. The x-axis represents the energy (GeV) and the y-axis represents the flux density. The plot shows the Crab pulsar's emission as seen by Fermi (radio to VHE) and VERITAS (VHE to TeV).

Conclusions and Future Prospects

Using the VERITAS and CRAB data, we have conducted a search for a correlation between the Crab pulsar's VHE emission and its radio giant pulses. We have also searched for LIV using VERITAS data on the Crab pulsar. The results of these searches are shown in Figures 1-3 and 4-5.

Acknowledgements

This work was supported by the National Science Foundation (NSF) Grant AST-0808012 and the Kavli Institute for Cosmological Physics. We thank the VERITAS and CRAB collaborations for their support and assistance.

References

1. A. Aleksic et al., *ApJ*, 738, 102 (2011)
2. A. Aleksic et al., *ApJ*, 738, 102 (2011)
3. A. Aleksic et al., *ApJ*, 738, 102 (2011)
4. A. Aleksic et al., *ApJ*, 738, 102 (2011)
5. A. Aleksic et al., *ApJ*, 738, 102 (2011)
6. A. Aleksic et al., *ApJ*, 738, 102 (2011)
7. A. Aleksic et al., *ApJ*, 738, 102 (2011)
8. A. Aleksic et al., *ApJ*, 738, 102 (2011)

MCCann

Crab Pulsar: Stereo Observations

- 73 hrs of data (Oct. 2009 - Mar. 2011) (Aleksić et al 2012)
- Energy range: $E > 50$ GeV
- Pulsation firmly detected
- H-Test (unbinned) : 6.4 σ
- EGRET-peaks (a-priori) : 7.7 σ
- Peaks get narrower w/energy
- New peak definitions $\pm 2\sigma$ FIT:
 - 8.8% of the whole phase
 - P1+P2: 10.4 σ , P1 5.5 σ , P2 9.9 σ
 - 3.4 σ hint at TW1 [0.04:0.14]
- P1/P2 ratio - 0.4 ± 0.2 at 100 GeV
- No significant yearly variability

Saito/Paneque

Pulsars

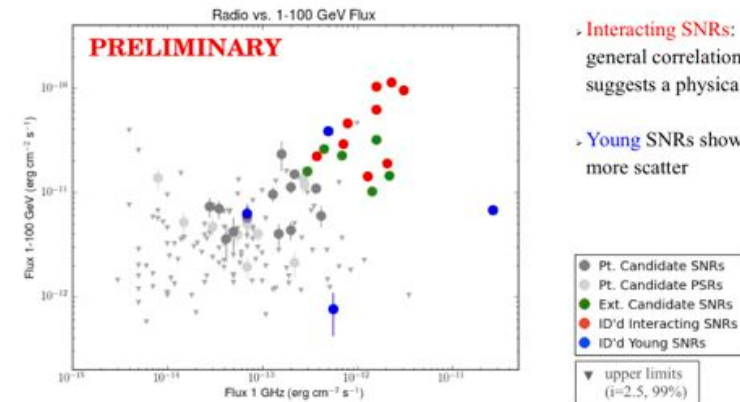
- Kerr on radio polarization measurements, Timokhin on theory of particle acceleration and gamma-ray production in pulsars

Supernova Remnants

- First Fermi LAT Catalog of SNRs – a sign that SNRs are a useful LAT population
 - Uniform analysis, including for systematic uncertainties related to the Galactic diffuse emission model (de Palma et al.)
 - Catalog will include analysis of LAT data with multiwavelength data from radio to TeV

Radio-GeV Correlation?

Radio synchrotron emission indicates the presence of relativistic leptons.
LAT-detected SNRs tend to be radio-bright:



T. J. Brandt

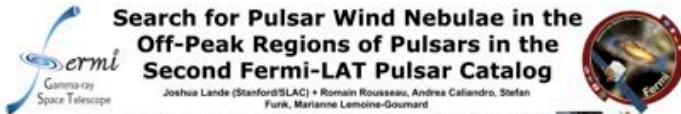
- Interacting SNRs: general correlation suggests a physical link
- Young SNRs show more scatter

Brandt

13

Pulsar Wind Nebulas

- Search for low-latitude >10 GeV LAT sources near HESS TeV sources



Summary: We performed a combined spectral and spatial analysis of the off-peak regions of LAT-detected pulsars and characterize the emission as being due to a pulsar wind, magnetospheric, or undetermined.

Abstract
We performed a search for new Pulsar Wind Nebulae (PWNe) in the regions surrounding LAT-detected pulsars. To perform this analysis, we selected all LAT-detected pulsars from the second Fermi-LAT pulsar catalog and searched for emission in their off-peak regions using 3 years of observations. To do this, we developed a Bayesian-block algorithm to define the off-peak. In the off-peak regions, we performed a combined spectral and spatial analysis to determine if the emission is due to a pulsar wind, is magnetospheric in nature, or is undetermined. We will present a description of our analysis method and preliminary results.

Lande

Introduction

Pulsars are magnetized rotating neutron stars, primarily characterized by their periodic emission. Pulsars are a major class of sources of GeV energies since the launch of the Large Area Telescope (LAT) on board the Fermi Gamma-ray Space Telescope (Fermi). The number of pulsars detected at GeV energies has rapidly increased.

Particles ejected from the pulsar can form a pulsar wind which can be observed over a broad spectrum of energies through its emission of synchrotron and inverse Compton radiation. This produces a Pulsar Wind Nebula (PWN) which is characterized by its spatially-extended and non-periodic emission. A growing number of PWNe have been observed at GeV energies.

The LAT collaboration is currently preparing a Second Fermi LAT Catalog of Gamma-ray Pulsars (2FC). Using 30 months of observations, 2FC will detail the analysis of 111 LAT-detected pulsars.

We searched for new PWNe detected in the regions surrounding LAT-detected pulsars. To do so, we developed an algorithm for selecting and removing the pulsed gamma-ray emission and searched for PWN emission in the off-peak regions.

Due to pulsar geometry, some pulsars can emit γ -rays over all pulsar phases. Therefore, we searched for and compared both PWN radiation and DC magnetospheric Pulsar emission.

Pulsar or PWN?

Spectral:

- Magnetospheric emission is expected to have an exponentially-cutoff spectrum. PWNe are expected to have a hard spectra at GeV energies.

Spatial:

- Pulsars are expected to be point-like while PWNe could be spatially extended.

Preliminary Results

- One particularly interesting region is PSR J1507-6420.

The emission is spatially/spectrally coincident with HESS J1359-640.

- This source is most likely a PWN associated with the pulsar.

Complicated Regions

- Some regions show significant emission but cannot be clearly identified as being magnetospheric or PWN.
- For example, PSR J1112-6103.

The spectrum is consistent with a soft power law.

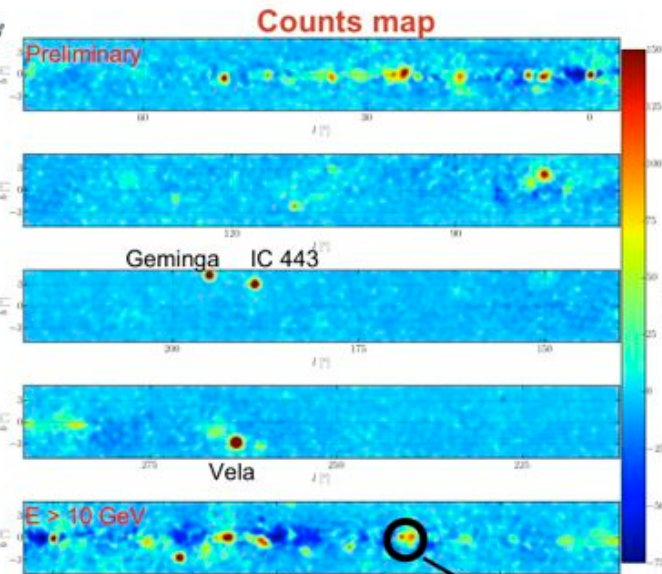
- If above emission that is firmly significantly extended, but appears to be a composite of multiple point-like sources.
- There is no clear way to classify this emission.

Off-peak Selection

We developed an algorithm to automatically select the off-peak emission in the regions of LAT-detected pulsars. The algorithm decomposes an energy and radius optimized pulsar light curve into Bayesian Blocks. The narrow Bayesian blocks (with 10% removed on either side) is selected to be the off-peak region.

Analysis Method

- We built an analysis pipeline to characterize the off-peak emission of all pulsars in 2FC.
- We used both the maximum-likelihood analysis packages *pointlike* and *gtlike*.
- We used *pointlike* to fit the position and test for extension of an assumed source in the off-peak region.
- We also used *pointlike* to compute test statistics maps and count-model counts maps of the region.
- We used *gtlike* to test the statistical significance of the assumed source and to fit the spectrum of the source.
- We used *gtlike* to compare a power-law spectral model to an exponentially-cutoff spectral model.
- For regions with no significant detection, we used *gtlike* to compute flux upper limits assuming both a power law and an exponentially cutoff spectrum.
- Full spectral and spatial results will be included in 2FC.



Galactic and Isotropic diffuses subtracted
Smoothed with a Gaussian of 0.27°



Rousseau

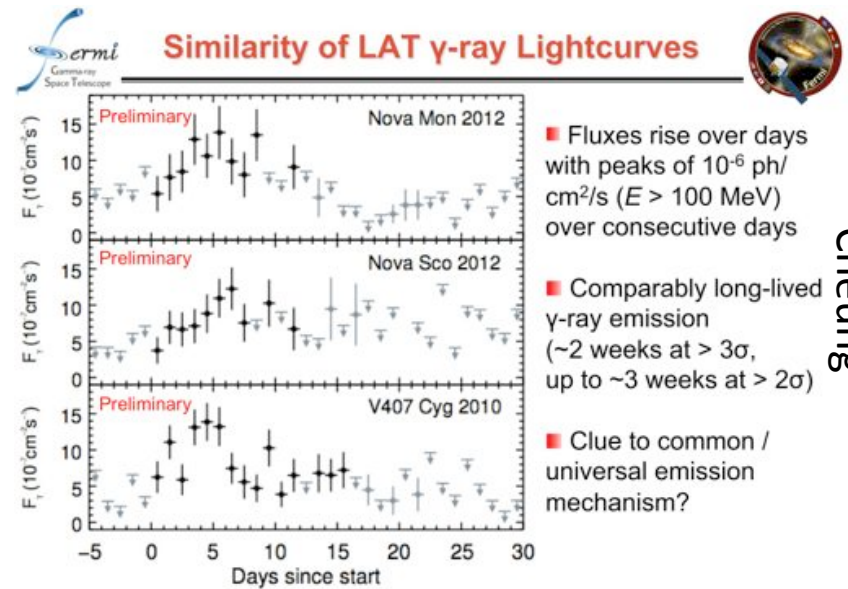
- Search for LAT sources in off-pulse regions of LAT pulsars
- Both involve spectral/spatial comparisons with HESS
- ~ 15 candidates found (large increment on known PWNe)

Other SNR/PWN studies

- Striani interpreted the LAT observations of the flaring Crab nebula in terms of flares and slower 'waves'

New Novas

- Two found since the 3rd FS
 - Unlike V407 Cyg (2010) they are of the much more common (but not recurrent) Classical Nova type
- In one case LAT detection preceded optical discovery (Cheung: LAT as a nova finder for $d < 4-6$ kpc)
- Martin & Dubus have been grappling with understanding the light curve and X-ray-to-gamma-ray spectrum of V407 Cyg

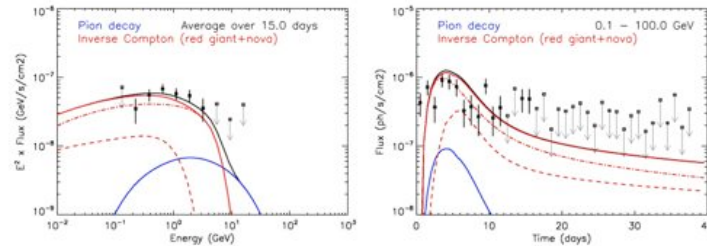


Cheung

V407 Cygni: Gamma-ray emission

- Parameters**
- $R_{\text{opt}} = 10$ AU
 - $\dot{M}_{\text{dot}} = 5 \cdot 10^{-8} M_{\odot}/\text{yr}$
 - $M_{\text{ej}} = 2 \cdot 10^{-6} M_{\odot}$
 - $V_{\text{ej}} = 3000$ km/s
 - $\eta_p = 5 \cdot 10^{-3}$, $\eta_e = 3 \cdot 10^{-4}$
 - $\xi = 3$
 - CDE 10^8 cm³ / 10AU

How matter accumulation around the WD helps...



Large reservoir of particles early on, close to nova photosphere
 Acceleration drops when shock exits the structure
 Bohm diffusion in upstream equipartition magnetic field

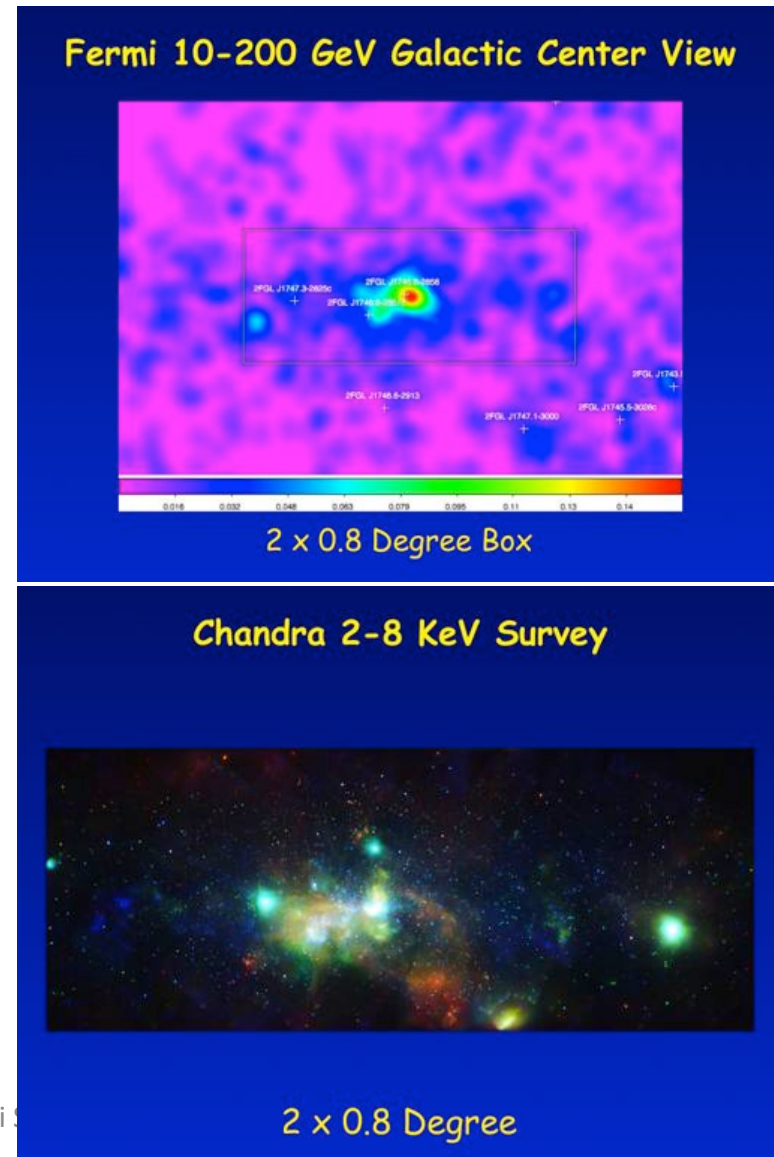
Martin

Galactic Center*

- Fred Baganoff gave beautiful talk on “the Fermi Galactic Zone of Avoidance”
 - Variety of X-ray evidence for potential gamma-ray sources – nonthermal filaments/shocks, PWNs, star-forming regions
- Looking forward to activity from the close approach of a $3 M_{\text{Earth}}$ cloud in Sept. 2013 [when you can use the word ‘peribothron’]

* More later

Summary 4th International Fermi

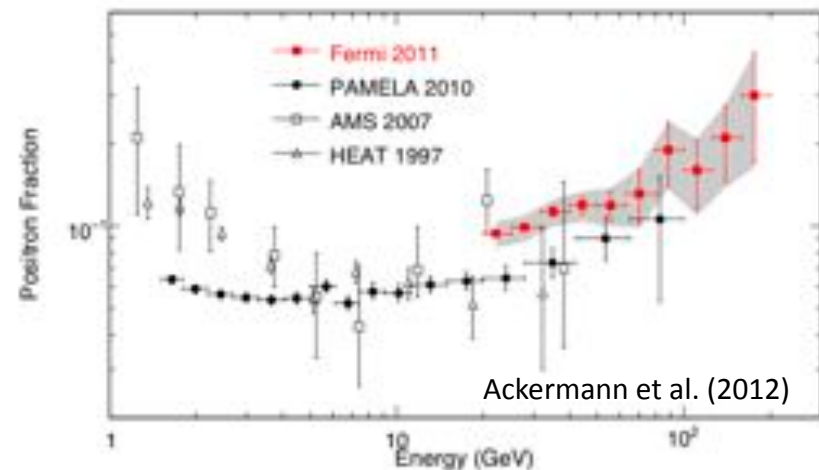


Baganoff

Cosmic Rays

- Stefano Profumo discussed interpretations of the rising positron fraction with energy (PAMELA result confirmed by LAT, preliminary results presented at 3rd FS)
 - Briefly: If it is dark matter it needs to be heavier than 200 GeV and have 100-1000 x $10^{-26} \text{ cm}^3 \text{ s}^{-1}$ annihilation rates
- “Any competent theoretician can fit any given theory to any given set of facts” (attrib. Redman)

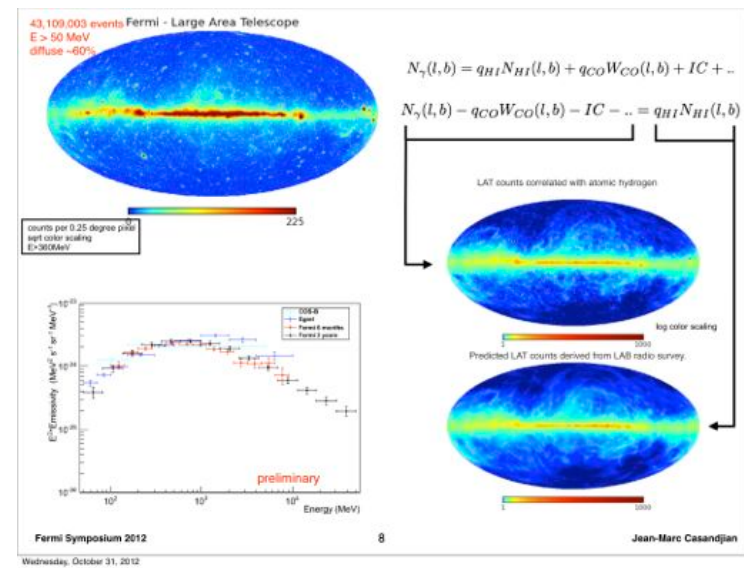
Positron Fraction



Kistler: CR $e^+ + e^-$ energy loss rate goes like E^2 (limits the number of sources that can contribute) & diffusion is along filaments (anisotropies do not necessarily point back to the sources)

Indirect Detection of Cosmic Rays

- Jean-Marc Casandjian presented a decomposition of the LAT gamma-ray observations into the component correlated with H I:
 - “Fermi-LAT is a beautiful instrument and perfect for what we want to measure”
 - Demonstrates that the force field approximation works well, and that the LAT provides enough statistical precision that you need to worry about, e.g., He and the accuracy of the gamma-ray production functions, in addition to electrons
- Chuck Dermer described issues, approaches, and preliminary results for the proton spectrum, including a break in the low-energy demodulated spectrum



Casandjian



Dermer

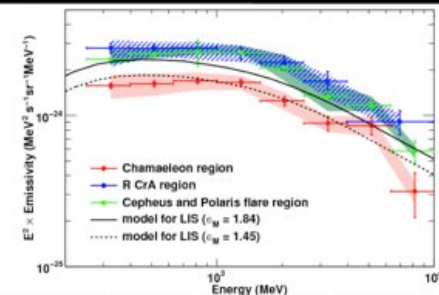
Indirect detection of CRs 2

- On scales of individual local interstellar clouds
LAT results indicate small but significant variations of CR density



Fermi Symposium, @Monterey, CA, Oct 31, 2012

CR Spectrum Close to the Solar System



Compare the HI emissivity spectra of each region with the LIS model

➤ LIS model: calculated from observed local interstellar spectrum assuming different nuclear enhancement factors (ϵ_M)

➤ Spectral shapes are similar among them.

➤ Emissivities differ by ~20% even if we consider the systematic uncertainties.

➔ Small (~20%) variation in local interstellar CR densities (if we assume uniform CR composition)

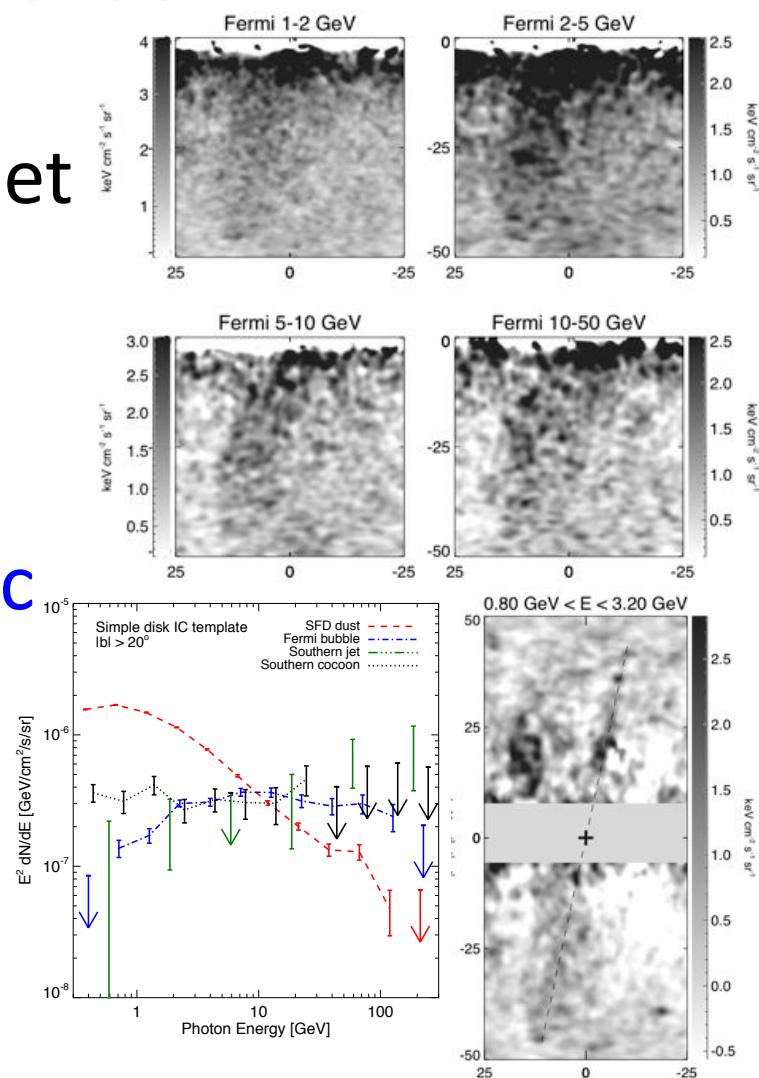
Katsuhiro Hayashi

Hayashi

9

Fermi Bubbles

- Pushing ahead: Cocoon & jet interpretation - “The jet might be even more dangerous than claiming a 130 GeV line at the Galactic center” (Finkbeiner)



Fermi Bubbles 2

- A LAT team analysis using template and Internal Linear Combination (template-free) approaches was also presented
- Analyses related to the Fermi Bubbles were also presented by Su and by Dobler

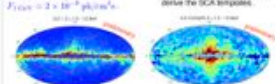
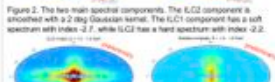
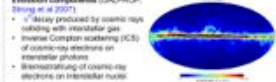
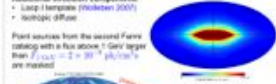


Fermi-LAT Gamma-ray Bubbles

Anna Franckowiak and Dmitry Malyshev (SLAC / KIPAC)
on behalf of the Fermi Large Area Telescope Collaboration



Summary: The Fermi bubbles (Su et al 2010) are two large structures in the Fermi-LAT gamma-ray data extending about 55 degrees above and below the Galactic center. We use two independent data analysis methods to study the Fermi bubbles. The first method is a novel method in diffuse gamma-ray data analysis. It is a generalization of the principal components analysis and the internal linear combinations method developed by the WMAP collaboration (Hinshaw et al 2007). The second method is a well established analysis procedure based on fitting templates to the gamma-ray data using gamma-ray emission model maps generated by the GALPROP code as the templates. The consistency between the results obtained with the two methods strengthens their robustness.

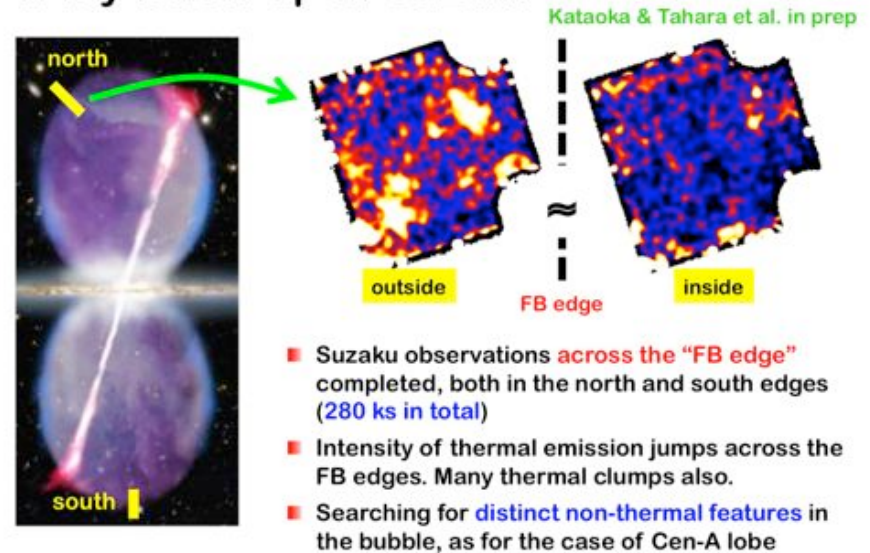
Spectral Components Analysis	Template Fitting
<p>The spectral components analysis (Malyshev 2012) is an internal data analysis method. The templates for the emission components are modeled as linear combinations of data maps in different energy bins, $\phi_i = \sum_j c_j \psi_j$, where i labels pixels and j labels energy bins.</p> $\phi_i = \sum_j c_j \psi_j$ <p>The data are linear combinations of templates up to index i:</p> $\phi_i = \sum_j c_j \psi_j$ <p>The linear decomposition coefficients c_j and the spectra ψ_j are found from a minimization of</p> $\chi^2 = \sum_i (\phi_i - \sum_j c_j \psi_j)^2$ <p>In the derivation of the templates we use the Fermi-LAT gamma-ray data, pass7, which covers between 1 GeV and 27 GeV, segmented in 7 energy bins and in pixels of approximately 2 deg size (HEALPix (Górski 2002) parameter mode = 32). We treat point sources from the second Fermi catalog (Dobler et al 2012) with flux above 1 GeV larger than $F_{1\text{GeV}} = 2 \times 10^{-5} \text{ ph/cm}^2/\text{s}$.</p>  <p>Figure 1. Gamma ray data used to derive the SCA templates.</p>  <p>Figure 2. The two main spectral components. The IC2 component is smoothed with a 2 deg Gaussian kernel. The IC1 component has a soft spectrum with index -2.7, while IC2 has a hard spectrum with index -2.2.</p>  <p>Figure 3. Model of the IC2 map with 2 Gaussians. The Gaussian extended in the Galactic latitude is used as a template for the Fermi bubbles to derive their spectrum (work in progress).</p>	<p>Method</p> <ol style="list-style-type: none"> 1. Perform all sky template fit with gamma-ray emission component templates. 2. Use residuals to the residual map to define a mask for the bubble region to avoid contamination of the bubble flux by other components. 3. Repeat all sky fit with bubble masked. 4. Use residuals to define bubble template -- bubble morphology. 5. Repeat all sky fit including bubble template -- bubble spectrum. <p>All sky template fit:</p> <p>A linear combination of templates is fitted to the count maps in 6 maximum likelihood procedure. The fit is performed in individual energy bins. For each energy bin the normalizations of the individual templates are free parameters. We use the quasi-Newton minimization algorithm.</p> <p>Emission components (GALPROP, Strong et al 2007):</p> <ul style="list-style-type: none"> • Decay produced by cosmic rays colliding with interstellar gas • Inverse Compton scattering (ICS) of cosmic-ray electrons on interstellar photons • Bremsstrahlung of cosmic-ray electrons on interstellar matter <p>Additional emission components:</p> <ul style="list-style-type: none"> • Loop 1 diffuse (Mackie 2007) • Isotropic diffuse <p>Point sources from the second Fermi catalog with a flux above 1 GeV larger than $F_{1\text{GeV}} = 2 \times 10^{-5} \text{ ph/cm}^2/\text{s}$ are treated.</p>  <p>Figure 4. IC1 and IC2 emission components obtained from GALPROP between 0 and 11 GeV.</p>  <p>Figure 5. Residual count map after performing the all sky fit. The bubble region and point sources were masked in the fit. Some of the substructures might be due to contribution of unmasked point sources (to be investigated).</p> <p>Study of Systematic Uncertainties:</p> <ul style="list-style-type: none"> • Systematic uncertainty on effective area • Systematic uncertainty introduced by choice of GALPROP model: selection of bubble template and corresponding spectrum is repeated for a number of GALPROP models
<p>Possible physical models and work in progress</p> <p>Possible sources:</p> <ol style="list-style-type: none"> 1. Jets from the black hole (Bier et al 2010; Cao et al 2011; Evrard et al 2011). 2. Wind from a starburst activity near the Galactic center (Cohen & Thompson 2011). 3. Stochastic acceleration in the Galactic halo (Sheng et al 2011; Mertsch & Sarkar 2011). <p>Work in progress:</p> <ol style="list-style-type: none"> 1. Spectral energy distribution of the bubbles. 2. Characterization of substructures and sharpness of the edges. 3. Systematic uncertainties. 	<p>References</p> <p>Cohen, M. et al. <i>ApJ</i> 719 (2010) L17 Cao, J. et al. <i>ApJ</i> 719 (2010) L17 Evrard, S. et al. <i>ApJ</i> 719 (2010) L17 Bier, J. et al. <i>ApJ</i> 719 (2010) L17 Mertsch, P. et al. <i>ApJ</i> 719 (2010) L17 Sheng, Z. et al. <i>ApJ</i> 719 (2010) L17 Thompson, T. et al. <i>ApJ</i> 719 (2010) L17 Dobler, D. et al. <i>ApJ</i> 719 (2010) L17 Su, M. et al. <i>ApJ</i> 719 (2010) L17 Mackie, R. et al. <i>ApJ</i> 719 (2010) L17 Mackie, R. et al. <i>ApJ</i> 719 (2010) L17</p>

Franckowiak & Malyshev

Fermi Bubbles 3

- Jun Kataoka showed Suzaku observations of the interior and exterior of the northern lobe and indicated that the MAXI >2 keV sky map is also being analyzed
- “There’s nothing like multiwavelength”
Finkbeiner

X-ray follow-up w/ Suzaku



24

Indirect Searches for Dark Matter

- More of a focus here than at 3rd Fermi Symposium
 - Dark Matter in the GC and Halo
 - Dark Matter in dSph galaxies
 - VERITAS Dark Matter Search
 - Dark Matter in Virgo?
 - 130-135 GeV Feature

Dark Matter in the GC and Halo

- Kevork Abazajian presented results consistent with a Dark Matter signal from the Galactic center region, and also consistent with plausible astrophysical sources
- Zaharijas reported limits from the inner Galaxy (excluding low latitudes) based on modeling and removing the Galactic diffuse foreground, marginalizing over some GALPROP parameters that are otherwise poorly constrained

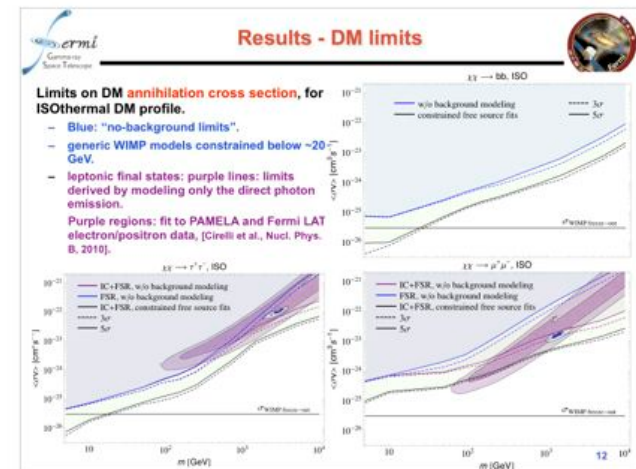
Abazajian

Zaharijas

Galactic Center Summary

Galactic Center has a new source consistent with extended emission.

- The source is has a **triplet of consistency with a dark matter annihilation source**:
 1. Morphology: NFW-like profile
 2. Rate: flux is consistent with the weak rate expected with thermal WIMP decoupling
 3. Spectrum: the spectrum is consistent with a broad range of particle masses, 10 GeV to 1 TeV, annihilating to $b\bar{b}$.
- The source is also consistent with the morphology, intensity and spectrum with **millisecond pulsars** existing in dense stellar clusters (e.g., globular clusters) and traced by LMXBs in Andromeda
- The source is also consistent with the morphology, intensity and spectrum of **electron cosmic-ray bremsstrahlung on molecular gas**, which is also mapped out by its synchrotron radio emission and the induced FeI 6.4 keV X-ray line (Yusef-Zadeh et al. 2012)



Dark Matter in dSphs

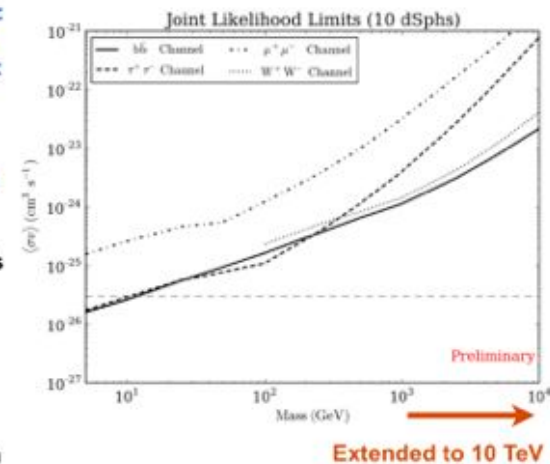
- Stacking analysis of dSph galaxies updated for 4 years and Pass 7, and careful explanation of the comparison with Pass 6 and expected statistical fluctuations
- See also contribution by Loparco on a model independent method for joint analysis



4-Year Pass7 Analysis



- Joint likelihood analysis of:
 - 10 dwarf galaxies
 - Expanded photon energy range: 100 MeV - 500 GeV
 - Constrain higher WIMP masses: 5 GeV - 10 TeV
 - Extended time period: 4 years
 - Improved instrument response: P7REPCLEAN_V9
- Model astrophysical backgrounds based on 2 years of Pass 7 data
 - 2FGL catalog sources (normalization free within 5')
 - 2-year diffuse background models (normalization free)
- Include statistical uncertainties in the solid-angle-integrated J-factor



Drica-Wagner

VERITAS Dark Matter Search

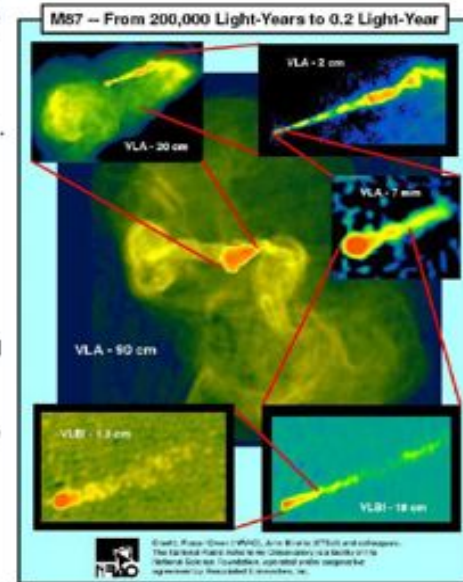
- VERITAS program was described by Geringer-Sameth – most sensitive in the $\sim > 200$ GeV WIMP mass range
 - 1 Galaxy cluster (Coma, 19 hr)
 - 2 Unassociated 2FGL sources (20 hr total), with 2 more planned for observation
 - 5 dSphs observed and plan to \sim triple the observing time on 3 of them (total $\sim > 200$ hr) and make a stacked analysis
 - Strong detection of the GC (SgrA*); plan a close-by halo study

No Dark Matter Signal from Virgo

- New since 3rd Fermi Symposium – a report by Han et al. (arXiv:1201.1003) of a detection of a broad emission region in Virgo consistent with a Dark Matter profile; superseded by Han et al. (arXiv: 1207.6749) no longer claiming this
- Gordon & Jogler presented independent LAT analyses of this region, reaching the same conclusions

Contaminants

- Point sources
 - E.g. active galactic nuclei (AGN) and star-burst galaxies.
 - Their spectra are usually modeled as power laws.
- Cosmic rays
 - Could produce detectable levels of gamma-rays in clusters.
 - Could be a spatially extended contaminant.
- Galactic and extra-galactic diffuse backgrounds.



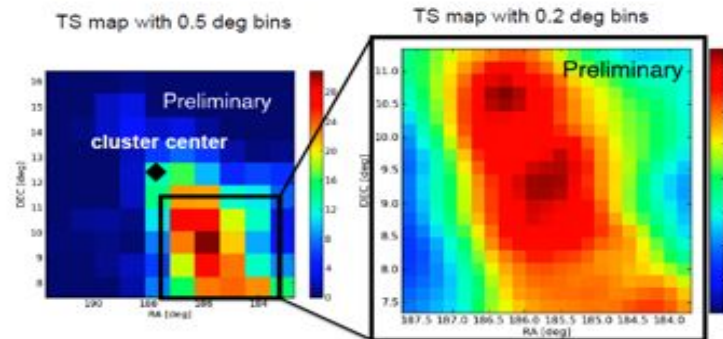
Gordon



Where does this emission come from?



If emission is caused by DM or Cosmic-rays it should be at the cluster center

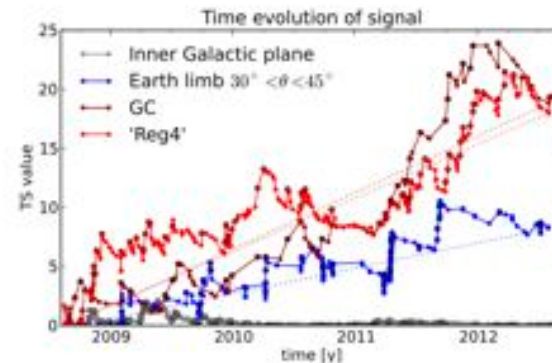


Jogler

Best source positions far offset from the cluster center!

130-135 GeV Feature

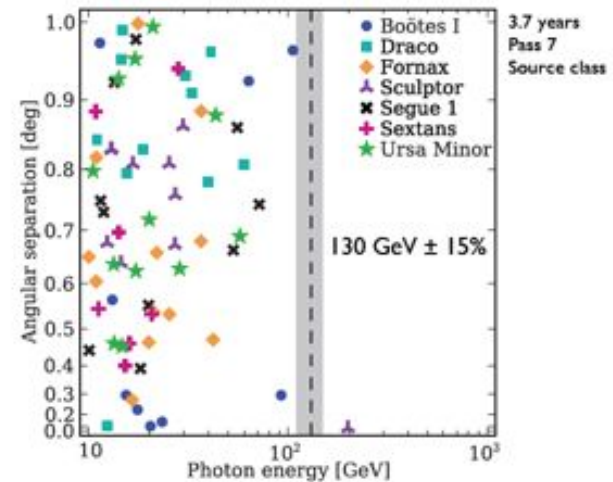
- New since the 3rd Fermi Symposium
- Presentations by Weniger (line search in the Galactic center), Albert (line search), Bloom (systematics from non-GC regions, Charles (potential instrumental effects in line searches), Koushiappas/Geringer-Sameth (line search in dSphs)



Finkbeiner, Su, & Weniger (arXiv:1209.4562)

Squeeze more information out of photons

e.g. line emission search from combined dwarfs



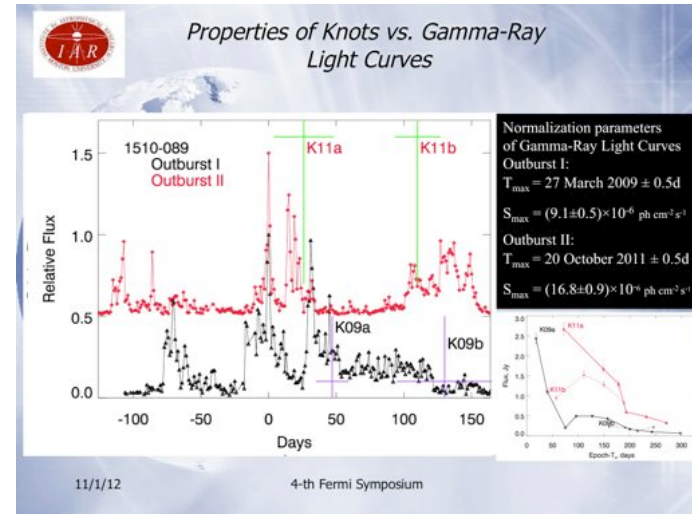
Geringer-Sameth and Koushiappas. PRD 86, 021302(R) (2012)

Koushiappas/Geringer-Sameth

Extragalactic

Active Galactic Nuclei

- Finke: “It seems that Fermi is a blazar machine”
- Gamma-ray flares appear to be correlated with the 43 GHz VLBI flux of the core
- F-GAMMA study of gamma-ray and cm-mm radio light curves finds strong correlations and results consistent with co-spatial emission regions on pc scales

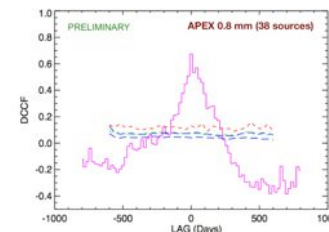


Jorstad

DCCF analysis First results



APEX sub-mm vs. Fermi/LAT (see poster by Larsson et al.)



- ⇒ mm/sub-mm and gamma-ray emission regions co-spatial (within the given uncertainties)
- ⇒ SED modeling: including the mm/sub-mm bands should be considered!

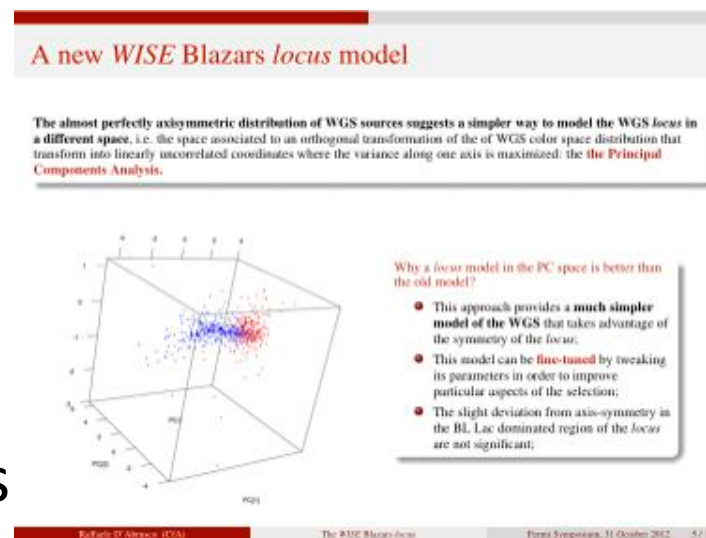
Larsson et al. in prep.

$\langle \text{lag} \rangle_{\text{sub-mm}}$: 7 +/- 7 days
 $\langle \text{lag} \rangle_{\text{sub-mm}}$ BL Lacs: -12 +/- 12 days
 $\langle \text{lag} \rangle_{\text{sub-mm}}$ FSRQs: 13 +/- 9 days

Fuhrmann

Active Galactic Nuclei 2

- The 500M+ source WISE infrared catalog has proven very powerful for finding blazars, which occupy a specific part of 3-color space
- In addition to a refinement of the implementation of the region, candidate associations for a number of 2FGL unassociated sources were presented (Massaro)



D'Abrusco

Active Galactic Nuclei 3

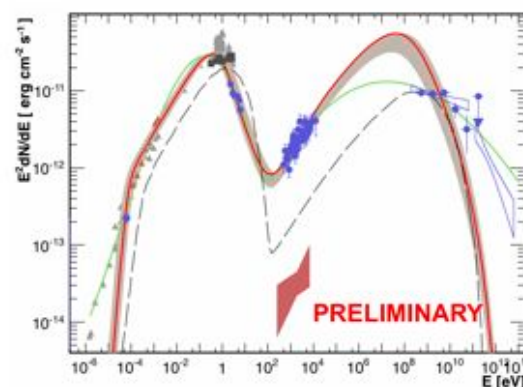
- The quality and quantity of LAT data are also spurring new directions in modeling



The end of the one zone leptonic model?



AP Librae – HESS & LAT detected ISP BL Lac



Extremely narrow
synchrotron component, very
broad (X-ray to TeV γ -ray)
Compton component

Cannot be fit with a one-zone
synchrotron/Compton model

Green curve: not a radiative
model fit, an empirical fit with
two 3rd degree polynomials

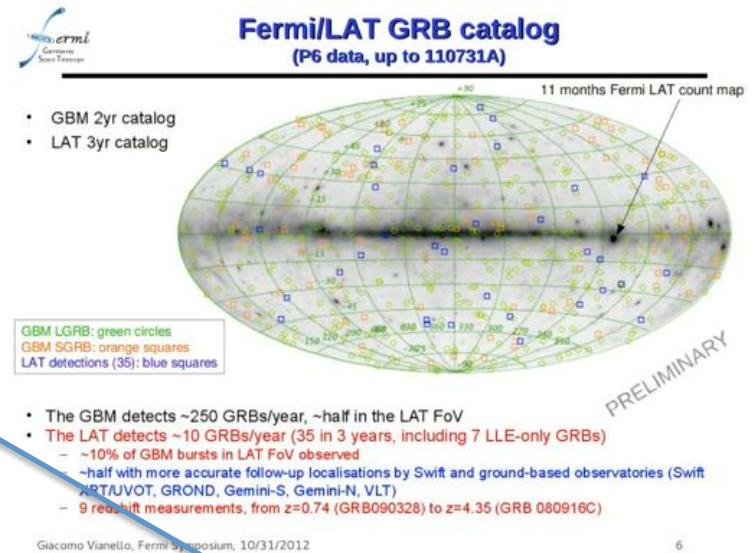
Finke

Abramowski et al. (in preparation)

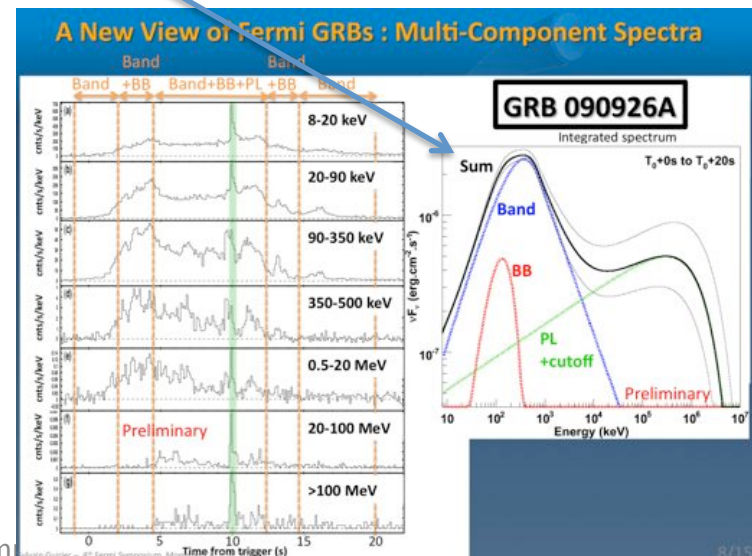
34

Gamma-Ray Bursts

- LAT has about 35 GRBs (vs. 1000+ for GBM)
- Band model** crisis: GBM + LAT spectra often require additional PL, cutoff PL, or thermal components to be well modeled
- The interpretations are not clear and would like to fit more physically motivated models (Vianello)
- The delays of the long-lasting LAT high-energy afterglows are difficult to explain
 - But these GRBs are useful for investigating Lorentz Invariance Violation from evaluating the time rate of change of the spectral index for GRBs over a range of redshifts (Guetta)
 - See also contribution by Vasileiou



Vianello



Guiriec

Gamma-Ray Bursts 2

- Preliminary Pass 8* analyses of LAT GRBs have recovered some additional (and in some cases more constraining) high-energy GRBs (**one with 28 GeV from GRB 080916C**)
- Simulations are now showing in detail how energy can be extracted from a spinning black hole with a thick accretion disk
 - All it takes is a **magnetic field and \$100** (Tchekhovskoy)
 - These studies indicate short-timescale QPO behavior near the end of the prompt phase – not clear yet whether this is detectable

* More later



New Fermi-LAT event reconstruction reveals more high-energy gamma rays from GRBs

Melissa Peuce-Rollins¹, Nicola Orlandi², and Jonathan Granot³
 on behalf of the Fermi Large Area Telescope Collaboration
¹INFN-Pisa ²Stanford University ³The Open University of Israel



Summary: Based on the experience gained during the first phase of the mission, the Fermi-LAT collaboration has undertaken a radical revision of the event level analysis. This revision affects the entire analysis scheme, from the Monte Carlo simulations to event reconstruction and background rejection. Although still under development, we can effectively benchmark the new event reconstruction in the special case of the prompt phase of bright Gamma-Ray Bursts (GRBs), where the signal to noise is large enough that loose selection cuts are sufficient to identify gamma rays associated with the source. Using the new tracker reconstruction and calorimeter clustering algorithms, we have re-analyzed ten GRBs previously detected by the LAT for which an α -ray/optical follow-up was possible and found four new photons with energies greater than 10 GeV in addition to the six previously known. Among these four is a 28 GeV photon from GRB 080916C, which has a redshift of 4.35, thus making it the highest known energy (>100 GeV) detected from a GRB. We present here the salient aspects of the new event reconstruction and discuss the scientific implications of these new high energy photons, such as constraining some extragalactic background light (EBL) models, the prompt emission mechanism and the bulk Lorentz factor of the emitting region.

Data selection

We concentrate on the 10 GRBs detected by the LAT with an α -ray/optical follow up \rightarrow reliable measurement, very accurate positioning

- $E > 10$ GeV when PSF returns nan to asymptotic value
- Remove obvious charged-particle events via ACD track the association
- Use events for which best track extrapolates to more than 4 X₀ of active material in CAL
- ROI set to 95% acceptance average PSF

Expect ~0.1 background events in a 90 s time window with this selection

Event reconstruction (Pass7 vs Pass8)

- Anti-Coincidence detector (ACD) [see Bahini, Poster]
 - Pass7: absolute distances between tracks and ACD hits
 - Pass8: Propagate covariance matrix, measure distances in units of sigma
- Tracker (TRK) [see Bahini, Poster]
 - Pass7: Pattern recognition seeded by CAL
 - Pass8: New pattern recognition decoupled from CAL
 - Global approach, common point seen as prefilter process
- Calorimeter (CAL) [see Sgiri, Poster]
 - Pass7: All crystal hits grouped together
 - Pass8: Clustering algorithm and subcluster classification (Fig. 1)

Spectral analysis

Complete Pass8 event level analysis not yet available

- Simulate GRBs with photonism using best fitted value for spectral index
- Normalise output with observed Pass7 SOURCE counts above 100 MeV
- Compute probability of observing the new photons

Probabilities suggest that these events are statistically consistent with photon spectrum derived with Pass7 [see tab. 1]

Variation on probability due to time evolution of spectral index estimated to be less than 35%

Results

Source Name	Unfitted	95% lower	95% upper	99% lower	99% upper
GRB 080916C	2.14	1.14	3.14	0.14	6.14
GRB 080916C	2.14	1.14	3.14	0.14	6.14
GRB 080916C	2.14	1.14	3.14	0.14	6.14
GRB 080916C	2.14	1.14	3.14	0.14	6.14
GRB 080916C	2.14	1.14	3.14	0.14	6.14
GRB 080916C	2.14	1.14	3.14	0.14	6.14
GRB 080916C	2.14	1.14	3.14	0.14	6.14
GRB 080916C	2.14	1.14	3.14	0.14	6.14
GRB 080916C	2.14	1.14	3.14	0.14	6.14
GRB 080916C	2.14	1.14	3.14	0.14	6.14

Table 1: Basic event topology information of the four new photons.

- 4 new photons with $E > 10$ GeV in addition to 6 previously detected
- All well within core PSF [see Fig. 2]
- Topology of these events is highly gamma-like [see tab. 12]
- Low probability of being BKG based on Monte Carlo simulations and event topology [see tab. 1]

Figure 2: Angular distance to source position for 4 new photons represented by solid vertical lines

Scientific interpretation

Figure 1: 28 GeV photon from GRB080916C in the LAT (α -ray orthogonal projection), reconstructed with Pass7 (right panel) with Pass8 (left panel). Events recovered thanks to the new CAL clustering algorithm.

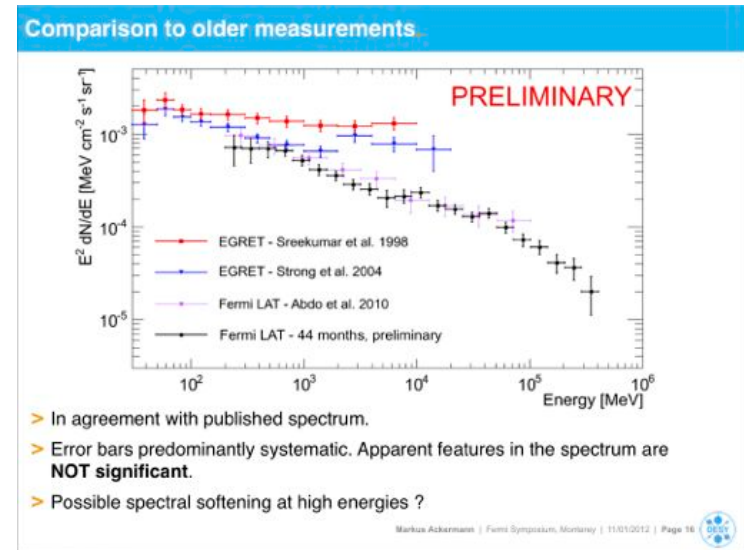
Figure 2: Predictions of optical depth from various EBL models. The four new photons are represented by the red stars.

- Synchrotron radiation challenged
 - Under certain assumptions, Γ factor can be as high as several 1000's ($\Gamma > 5000$ for GRB080916C and $\Gamma > 2000$ for GRB 080414A)
 - See however, Kumar et al. 2012
- Tighter constraints on the Extragalactic Background Light (EBL)
 - GRB080916C photon ($z = 4.35$) most constraining so far (Fig. 3)
- Lorentz invariance violation (LIV)
 - Constraints on linear LIV from 27.5 GeV photon from GRB080916C: 11% weaker than 10 GeV photon

Peuce-Rollins

Extragalactic Diffuse Background

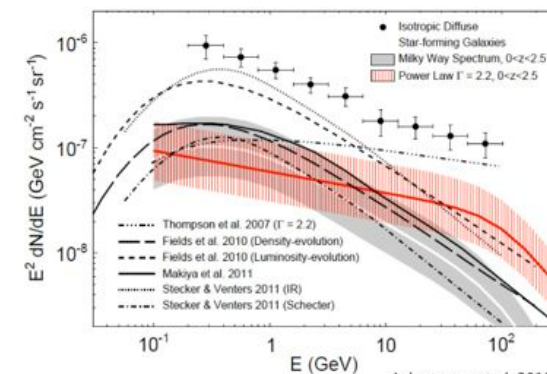
- Markus Ackermann presented an updated LAT analysis (44 months, 200 MeV to 410 GeV)
- Decomposition into contributions from various source classes remains a hot and important topic
 - See contributions by Chakraborty, Donato, Inoue, & Storm on star-forming galaxies, MAGN, and galaxy clusters
- Also thank Michael Shaw for his blazar redshift survey



Ackermann

IGRB CONTRIBUTION

Contribution by unresolved star-forming galaxies is comparable to that of blazars
4-23% of LAT-measured isotropic diffuse intensity >0.1 GeV



Bechtol

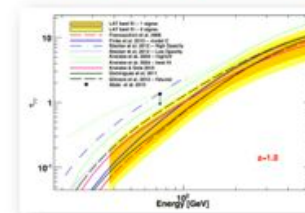
Extragalactic Background Light

- Much progress since 3rd Fermi Symposium, in terms of analysis approaches and data
- LAT composite analysis of 150 gamma-ray bright BL Lacs, fitting scale factors for various published EBL models
- HESS measurements of EBL density (IR) at low redshift has better sensitivity than the LAT (contrib. by Giebels)
- Related contributions on the IGMF by Arlen, Venters, & Vovk



Composite Likelihood Results: 2

- A significant steepening in the blazars' spectra is detected
- This is consistent with that expected by a 'minimal' EBL:
 - i.e. EBL at the level of galaxy counts
 - 4 models rejected above 3sigma
- All the non-rejected models yield a significance of detection of 5.6-5.9 σ
- The level of EBL is 3-4 times lower than our previous UL (Abdo+10, ApJ 723, 1082)

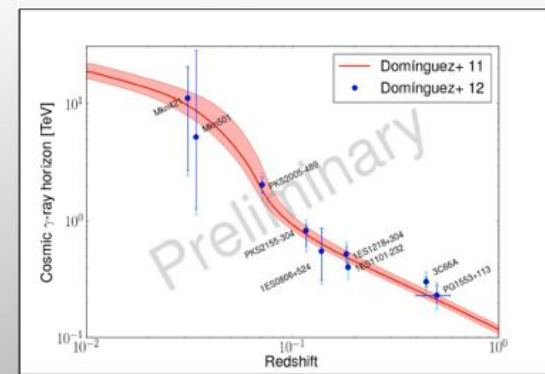


Ackermann+12

Model*	Ref**	Significance of best Rejection†	χ^2	Significance of best Rejection†
Stocker et al. (2006) - fast evolution	(27)	4.6	0.93±0.02	17.3
Stocker et al. (2006) - baseline	(27)	4.6	0.12±0.03	15.3
Krauss et al. (2004) - high UV	(22)	5.1	0.37±0.08	5.9
Krauss et al. (2004) - best fit	(22)	5.8	0.53±0.12	3.2
Gilmore et al. (2012) - fiducial	(25)	5.8	0.67±0.14	1.9
Primack et al. (2007)	(56)	5.5	0.77±0.15	1.2
Dominguez et al. (2011)	(25)	5.9	1.02±0.23	1.1
Finkbeiner et al. (2010) - model C	(34)	5.8	0.86±0.23	1.0
Franceschini et al. (2008)	(7)	5.9	1.02±0.23	0.9
Gilmore et al. (2012) - best	(25)	5.8	1.02±0.22	0.7
Krauss & Diehl (2010)	(26)	5.7	0.80±0.19	0.6
Gilmore et al. (2006) - fiducial	(2)	5.8	0.99±0.22	0.6

Ajello

Cosmic γ -ray Horizon: results



There are 4 out of 15 cases where our maximum likelihood methodology could not be applied since the prediction from the synchrotron/SSC model was lower than the detected flux by the Cherenkov telescopes.

Two other cases where the statistical uncertainties were too high to set any constraint on EBL.

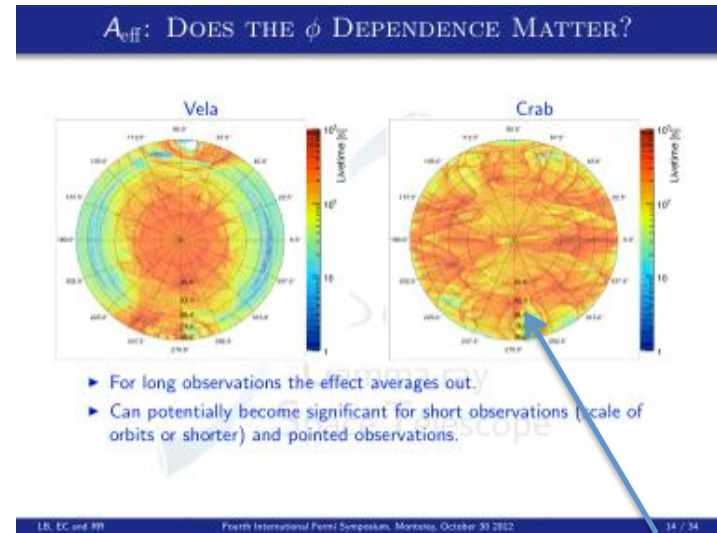
Dominguez

LAT Performance

Pass 7 & Pass 7 Reprocessing

- Since the 3rd Fermi Symposium the LAT Collaboration has moved to Pass 7 event selections
 - Not a new reconstruction but important improvements in classification (e.g., for increased A_{eff} at low energies)
- Luca Baldini summarized the recent LAT publication on the Pass 7 performance for high-level analysis. A Great Read*
- Now a Pass 7 reprocessing has been undertaken to update calibration constants, affecting energy scale and PSF (for the better)
 - First results presented this week
 - See also Wood & Roth poster on the inflight PSF fitting
 - Release by the end of the year

* arXiv:[1206.1896](https://arxiv.org/abs/1206.1896)



Baldini

(N.B. edge of FOV is at 3rd ring)

Fermi LAT data reprocessed with updated calibration constants

John D'Amico and Eric Charles
on behalf of the Fermi LAT Telescope Collaboration
Istituto Nazionale di Fisica Nucleare, sezione di Pisa, Italy
SLAC National Accelerator Laboratory, Menlo Park CA, USA

Summary: The first four years of the Fermi LAT data have been reprocessed with updated calibration constants leading to improved data quality and reduced systematic uncertainties.

Four years into the mission, the understanding of the Fermi LAT detectors properties and data analysis is now far beyond the original commissioning. Thanks to a careful analysis of flight data, we were able to trace back some of our major sources of systematic uncertainties to the end of the original calibration constants for some of the detectors. In this paper, we report a major collaboration effort to update these constants, to use them to reprocess the first 4 years of raw data, and the improvements obtained for low and high energy analysis. The Pass 7 reprocessed data, also known as Pass 7 'P7', 'P7R', 'P7D', 'P7C', 'P7E', 'P7F', 'P7G', 'P7H', 'P7I', 'P7J', 'P7K', 'P7L', 'P7M', 'P7N', 'P7O', 'P7P', 'P7Q', 'P7R', 'P7S', 'P7T', 'P7U', 'P7V', 'P7W', 'P7X', 'P7Y', 'P7Z', 'P7AA', 'P7AB', 'P7AC', 'P7AD', 'P7AE', 'P7AF', 'P7AG', 'P7AH', 'P7AI', 'P7AJ', 'P7AK', 'P7AL', 'P7AM', 'P7AN', 'P7AO', 'P7AP', 'P7AQ', 'P7AR', 'P7AS', 'P7AT', 'P7AU', 'P7AV', 'P7AW', 'P7AX', 'P7AY', 'P7AZ', 'P7BA', 'P7BB', 'P7BC', 'P7BD', 'P7BE', 'P7BF', 'P7BG', 'P7BH', 'P7BI', 'P7BJ', 'P7BK', 'P7BL', 'P7BM', 'P7BN', 'P7BO', 'P7BP', 'P7BQ', 'P7BR', 'P7BS', 'P7BT', 'P7BU', 'P7BV', 'P7BW', 'P7BX', 'P7BY', 'P7BZ', 'P7CA', 'P7CB', 'P7CC', 'P7CD', 'P7CE', 'P7CF', 'P7CG', 'P7CH', 'P7CI', 'P7CJ', 'P7CK', 'P7CL', 'P7CM', 'P7CN', 'P7CO', 'P7CP', 'P7CQ', 'P7CR', 'P7CS', 'P7CT', 'P7CU', 'P7CV', 'P7CW', 'P7CX', 'P7CY', 'P7CZ', 'P7DA', 'P7DB', 'P7DC', 'P7DD', 'P7DE', 'P7DF', 'P7DG', 'P7DH', 'P7DI', 'P7DJ', 'P7DK', 'P7DL', 'P7DM', 'P7DN', 'P7DO', 'P7DP', 'P7DQ', 'P7DR', 'P7DS', 'P7DT', 'P7DU', 'P7DV', 'P7DW', 'P7DX', 'P7DY', 'P7DZ', 'P7EA', 'P7EB', 'P7EC', 'P7ED', 'P7EE', 'P7EF', 'P7EG', 'P7EH', 'P7EI', 'P7EJ', 'P7EK', 'P7EL', 'P7EM', 'P7EN', 'P7EO', 'P7EP', 'P7EQ', 'P7ER', 'P7ES', 'P7ET', 'P7EU', 'P7EV', 'P7EW', 'P7EX', 'P7EY', 'P7EZ', 'P7FA', 'P7FB', 'P7FC', 'P7FD', 'P7FE', 'P7FF', 'P7FG', 'P7FH', 'P7FI', 'P7FJ', 'P7FK', 'P7FL', 'P7FM', 'P7FN', 'P7FO', 'P7FP', 'P7FQ', 'P7FR', 'P7FS', 'P7FT', 'P7FU', 'P7FV', 'P7FW', 'P7FX', 'P7FY', 'P7FZ', 'P7GA', 'P7GB', 'P7GC', 'P7GD', 'P7GE', 'P7GF', 'P7GG', 'P7GH', 'P7GI', 'P7GJ', 'P7GK', 'P7GL', 'P7GM', 'P7GN', 'P7GO', 'P7GP', 'P7GQ', 'P7GR', 'P7GS', 'P7GT', 'P7GU', 'P7GV', 'P7GW', 'P7GX', 'P7GY', 'P7GZ', 'P7HA', 'P7HB', 'P7HC', 'P7HD', 'P7HE', 'P7HF', 'P7HG', 'P7HH', 'P7HI', 'P7HJ', 'P7HK', 'P7HL', 'P7HM', 'P7HN', 'P7HO', 'P7HP', 'P7HQ', 'P7HR', 'P7HS', 'P7HT', 'P7HU', 'P7HV', 'P7HW', 'P7HX', 'P7HY', 'P7HZ', 'P7IA', 'P7IB', 'P7IC', 'P7ID', 'P7IE', 'P7IF', 'P7IG', 'P7IH', 'P7II', 'P7IJ', 'P7IK', 'P7IL', 'P7IM', 'P7IN', 'P7IO', 'P7IP', 'P7IQ', 'P7IR', 'P7IS', 'P7IT', 'P7IU', 'P7IV', 'P7IW', 'P7IX', 'P7IY', 'P7IZ', 'P7JA', 'P7JB', 'P7JC', 'P7JD', 'P7JE', 'P7JF', 'P7JG', 'P7JH', 'P7JI', 'P7JJ', 'P7JK', 'P7JL', 'P7JM', 'P7JN', 'P7JO', 'P7JP', 'P7JQ', 'P7JR', 'P7JS', 'P7JT', 'P7JU', 'P7JV', 'P7JW', 'P7JX', 'P7JY', 'P7JZ', 'P7KA', 'P7KB', 'P7KC', 'P7KD', 'P7KE', 'P7KF', 'P7KG', 'P7KH', 'P7KI', 'P7KJ', 'P7KK', 'P7KL', 'P7KM', 'P7KN', 'P7KO', 'P7KP', 'P7KQ', 'P7KR', 'P7KS', 'P7KT', 'P7KU', 'P7KV', 'P7KW', 'P7KX', 'P7KY', 'P7KZ', 'P7LA', 'P7LB', 'P7LC', 'P7LD', 'P7LE', 'P7LF', 'P7LG', 'P7LH', 'P7LI', 'P7LJ', 'P7LK', 'P7LL', 'P7LM', 'P7LN', 'P7LO', 'P7LP', 'P7LQ', 'P7LR', 'P7LS', 'P7LT', 'P7LU', 'P7LV', 'P7LW', 'P7LX', 'P7LY', 'P7LZ', 'P7MA', 'P7MB', 'P7MC', 'P7MD', 'P7ME', 'P7MF', 'P7MG', 'P7MH', 'P7MI', 'P7MJ', 'P7MK', 'P7ML', 'P7MM', 'P7MN', 'P7MO', 'P7MP', 'P7MQ', 'P7MR', 'P7MS', 'P7MT', 'P7MU', 'P7MV', 'P7MW', 'P7MX', 'P7MY', 'P7MZ', 'P7NA', 'P7NB', 'P7NC', 'P7ND', 'P7NE', 'P7NF', 'P7NG', 'P7NH', 'P7NI', 'P7NJ', 'P7NK', 'P7NL', 'P7NM', 'P7NN', 'P7NO', 'P7NP', 'P7NQ', 'P7NR', 'P7NS', 'P7NT', 'P7NU', 'P7NV', 'P7NW', 'P7NX', 'P7NY', 'P7NZ', 'P7OA', 'P7OB', 'P7OC', 'P7OD', 'P7OE', 'P7OF', 'P7OG', 'P7OH', 'P7OI', 'P7OJ', 'P7OK', 'P7OL', 'P7OM', 'P7ON', 'P7OO', 'P7OP', 'P7OQ', 'P7OR', 'P7OS', 'P7OT', 'P7OU', 'P7OV', 'P7OW', 'P7OX', 'P7OY', 'P7OZ', 'P7PA', 'P7PB', 'P7PC', 'P7PD', 'P7PE', 'P7PF', 'P7PG', 'P7PH', 'P7PI', 'P7PJ', 'P7PK', 'P7PL', 'P7PM', 'P7PN', 'P7PO', 'P7PP', 'P7PQ', 'P7PR', 'P7PS', 'P7PT', 'P7PU', 'P7PV', 'P7PW', 'P7PX', 'P7PY', 'P7PZ', 'P7QA', 'P7QB', 'P7QC', 'P7QD', 'P7QE', 'P7QF', 'P7QG', 'P7QH', 'P7QI', 'P7QJ', 'P7QK', 'P7QL', 'P7QM', 'P7QN', 'P7QO', 'P7QP', 'P7QQ', 'P7QR', 'P7QS', 'P7QT', 'P7QU', 'P7QV', 'P7QW', 'P7QX', 'P7QY', 'P7QZ', 'P7RA', 'P7RB', 'P7RC', 'P7RD', 'P7RE', 'P7RF', 'P7RG', 'P7RH', 'P7RI', 'P7RJ', 'P7RK', 'P7RL', 'P7RM', 'P7RN', 'P7RO', 'P7RP', 'P7RQ', 'P7RR', 'P7RS', 'P7RT', 'P7RU', 'P7RV', 'P7RW', 'P7RX', 'P7RY', 'P7RZ', 'P7SA', 'P7SB', 'P7SC', 'P7SD', 'P7SE', 'P7SF', 'P7SG', 'P7SH', 'P7SI', 'P7SJ', 'P7SK', 'P7SL', 'P7SM', 'P7SN', 'P7SO', 'P7SP', 'P7SQ', 'P7SR', 'P7SS', 'P7ST', 'P7SU', 'P7SV', 'P7SW', 'P7SX', 'P7SY', 'P7SZ', 'P7TA', 'P7TB', 'P7TC', 'P7TD', 'P7TE', 'P7TF', 'P7TG', 'P7TH', 'P7TI', 'P7TJ', 'P7TK', 'P7TL', 'P7TM', 'P7TN', 'P7TO', 'P7TP', 'P7TQ', 'P7TR', 'P7TS', 'P7TT', 'P7TU', 'P7TV', 'P7TW', 'P7TX', 'P7TY', 'P7TZ', 'P7UA', 'P7UB', 'P7UC', 'P7UD', 'P7UE', 'P7UF', 'P7UG', 'P7UH', 'P7UI', 'P7UJ', 'P7UK', 'P7UL', 'P7UM', 'P7UN', 'P7UO', 'P7UP', 'P7UQ', 'P7UR', 'P7US', 'P7UT', 'P7UU', 'P7UV', 'P7UW', 'P7UX', 'P7UY', 'P7UZ', 'P7VA', 'P7VB', 'P7VC', 'P7VD', 'P7VE', 'P7VF', 'P7VG', 'P7VH', 'P7VI', 'P7VJ', 'P7VK', 'P7VL', 'P7VM', 'P7VN', 'P7VO', 'P7VP', 'P7VQ', 'P7VR', 'P7VS', 'P7VT', 'P7VU', 'P7VV', 'P7VW', 'P7VX', 'P7VY', 'P7VZ', 'P7WA', 'P7WB', 'P7WC', 'P7WD', 'P7WE', 'P7WF', 'P7WG', 'P7WH', 'P7WI', 'P7WJ', 'P7WK', 'P7WL', 'P7WM', 'P7WN', 'P7WO', 'P7WP', 'P7WQ', 'P7WR', 'P7WS', 'P7WT', 'P7WU', 'P7WV', 'P7WW', 'P7WX', 'P7WY', 'P7WZ', 'P7XA', 'P7XB', 'P7XC', 'P7XD', 'P7XE', 'P7XF', 'P7XG', 'P7XH', 'P7XI', 'P7XJ', 'P7XK', 'P7XL', 'P7XM', 'P7XN', 'P7XO', 'P7XP', 'P7XQ', 'P7XR', 'P7XS', 'P7XT', 'P7XU', 'P7XV', 'P7XW', 'P7XX', 'P7XY', 'P7XZ', 'P7YA', 'P7YB', 'P7YC', 'P7YD', 'P7YE', 'P7YF', 'P7YG', 'P7YH', 'P7YI', 'P7YJ', 'P7YK', 'P7YL', 'P7YM', 'P7YN', 'P7YO', 'P7YP', 'P7YQ', 'P7YR', 'P7YS', 'P7YT', 'P7YU', 'P7YV', 'P7YW', 'P7YX', 'P7YY', 'P7YZ', 'P7ZA', 'P7ZB', 'P7ZC', 'P7ZD', 'P7ZE', 'P7ZF', 'P7ZG', 'P7ZH', 'P7ZI', 'P7ZJ', 'P7ZK', 'P7ZL', 'P7ZM', 'P7ZN', 'P7ZO', 'P7ZP', 'P7ZQ', 'P7ZR', 'P7ZS', 'P7ZT', 'P7ZU', 'P7ZV', 'P7ZW', 'P7ZX', 'P7ZY', 'P7ZZ', 'P7AA', 'P7AB', 'P7AC', 'P7AD', 'P7AE', 'P7AF', 'P7AG', 'P7AH', 'P7AI', 'P7AJ', 'P7AK', 'P7AL', 'P7AM', 'P7AN', 'P7AO', 'P7AP', 'P7AQ', 'P7AR', 'P7AS', 'P7AT', 'P7AU', 'P7AV', 'P7AW', 'P7AX', 'P7AY', 'P7AZ', 'P7BA', 'P7BB', 'P7BC', 'P7BD', 'P7BE', 'P7BF', 'P7BG', 'P7BH', 'P7BI', 'P7BJ', 'P7BK', 'P7BL', 'P7BM', 'P7BN', 'P7BO', 'P7BP', 'P7BQ', 'P7BR', 'P7BS', 'P7BT', 'P7BU', 'P7BV', 'P7BW', 'P7BX', 'P7BY', 'P7BZ', 'P7CA', 'P7CB', 'P7CC', 'P7CD', 'P7CE', 'P7CF', 'P7CG', 'P7CH', 'P7CI', 'P7CJ', 'P7CK', 'P7CL', 'P7CM', 'P7CN', 'P7CO', 'P7CP', 'P7CQ', 'P7CR', 'P7CS', 'P7CT', 'P7CU', 'P7CV', 'P7CW', 'P7CX', 'P7CY', 'P7CZ', 'P7DA', 'P7DB', 'P7DC', 'P7DD', 'P7DE', 'P7DF', 'P7DG', 'P7DH', 'P7DI', 'P7DJ', 'P7DK', 'P7DL', 'P7DM', 'P7DN', 'P7DO', 'P7DP', 'P7DQ', 'P7DR', 'P7DS', 'P7DT', 'P7DU', 'P7DV', 'P7DW', 'P7DX', 'P7DY', 'P7DZ', 'P7EA', 'P7EB', 'P7EC', 'P7ED', 'P7EE', 'P7EF', 'P7EG', 'P7EH', 'P7EI', 'P7EJ', 'P7EK', 'P7EL', 'P7EM', 'P7EN', 'P7EO', 'P7EP', 'P7EQ', 'P7ER', 'P7ES', 'P7ET', 'P7EU', 'P7EV', 'P7EW', 'P7EX', 'P7EY', 'P7EZ', 'P7FA', 'P7FB', 'P7FC', 'P7FD', 'P7FE', 'P7FF', 'P7FG', 'P7FH', 'P7FI', 'P7FJ', 'P7FK', 'P7FL', 'P7FM', 'P7FN', 'P7FO', 'P7FP', 'P7FQ', 'P7FR', 'P7FS', 'P7FT', 'P7FU', 'P7FV', 'P7FW', 'P7FX', 'P7FY', 'P7FZ', 'P7GA', 'P7GB', 'P7GC', 'P7GD', 'P7GE', 'P7GF', 'P7GG', 'P7GH', 'P7GI', 'P7GJ', 'P7GK', 'P7GL', 'P7GM', 'P7GN', 'P7GO', 'P7GP', 'P7GQ', 'P7GR', 'P7GS', 'P7GT', 'P7GU', 'P7GV', 'P7GW', 'P7GX', 'P7GY', 'P7GZ', 'P7HA', 'P7HB', 'P7HC', 'P7HD', 'P7HE', 'P7HF', 'P7HG', 'P7HH', 'P7HI', 'P7HJ', 'P7HK', 'P7HL', 'P7HM', 'P7HN', 'P7HO', 'P7HP', 'P7HQ', 'P7HR', 'P7HS', 'P7HT', 'P7HU', 'P7HV', 'P7HW', 'P7HX', 'P7HY', 'P7HZ', 'P7IA', 'P7IB', 'P7IC', 'P7ID', 'P7IE', 'P7IF', 'P7IG', 'P7IH', 'P7II', 'P7IJ', 'P7IK', 'P7IL', 'P7IM', 'P7IN', 'P7IO', 'P7IP', 'P7IQ', 'P7IR', 'P7IS', 'P7IT', 'P7IU', 'P7IV', 'P7IW', 'P7IX', 'P7IY', 'P7IZ', 'P7JA', 'P7JB', 'P7JC', 'P7JD', 'P7JE', 'P7JF', 'P7JG', 'P7JH', 'P7JI', 'P7JJ', 'P7JK', 'P7JL', 'P7JM', 'P7JN', 'P7JO', 'P7JP', 'P7JQ', 'P7JR', 'P7JS', 'P7JT', 'P7JU', 'P7JV', 'P7JW', 'P7JX', 'P7JY', 'P7JZ', 'P7KA', 'P7KB', 'P7KC', 'P7KD', 'P7KE', 'P7KF', 'P7KG', 'P7KH', 'P7KI', 'P7KJ', 'P7KL', 'P7KM', 'P7KN', 'P7KO', 'P7KP', 'P7KQ', 'P7KR', 'P7KS', 'P7KT', 'P7KU', 'P7KV', 'P7KW', 'P7KX', 'P7KY', 'P7KZ', 'P7LA', 'P7LB', 'P7LC', 'P7LD', 'P7LE', 'P7LF', 'P7LG', 'P7LH', 'P7LI', 'P7LJ', 'P7LK', 'P7LL', 'P7LM', 'P7LN', 'P7LO', 'P7LP', 'P7LQ', 'P7LR', 'P7LS', 'P7LT', 'P7LU', 'P7LV', 'P7LW', 'P7LX', 'P7LY', 'P7LZ', 'P7MA', 'P7MB', 'P7MC', 'P7MD', 'P7ME', 'P7MF', 'P7MG', 'P7MH', 'P7MI', 'P7MJ', 'P7MK', 'P7ML', 'P7MM', 'P7MN', 'P7MO', 'P7MP', 'P7MQ', 'P7MR', 'P7MS', 'P7MT', 'P7MU', 'P7MV', 'P7MW', 'P7MX', 'P7MY', 'P7MZ', 'P7NA', 'P7NB', 'P7NC', 'P7ND', 'P7NE', 'P7NF', 'P7NG', 'P7NH', 'P7NI', 'P7NJ', 'P7NK', 'P7NL', 'P7NM', 'P7NN', 'P7NO', 'P7NP', 'P7NQ', 'P7NR', 'P7NS', 'P7NT', 'P7NU', 'P7NV', 'P7NW', 'P7NX', 'P7NY', 'P7NZ', 'P7OA', 'P7OB', 'P7OC', 'P7OD', 'P7OE', 'P7OF', 'P7OG', 'P7OH', 'P7OI', 'P7OJ', 'P7OK', 'P7OL', 'P7OM', 'P7ON', 'P7OO', 'P7OP', 'P7OQ', 'P7OR', 'P7OS', 'P7OT', 'P7OU', 'P7OV', 'P7OW', 'P7OX', 'P7OY', 'P7OZ', 'P7PA', 'P7PB', 'P7PC', 'P7PD', 'P7PE', 'P7PF', 'P7PG', 'P7PH', 'P7PI', 'P7PJ', 'P7PK', 'P7PL', 'P7PM', 'P7PN', 'P7PO', 'P7PP', 'P7PQ', 'P7PR', 'P7PS', 'P7PT', 'P7PU', 'P7PV', 'P7PW', 'P7PX', 'P7PY', 'P7PZ', 'P7QA', 'P7QB', 'P7QC', 'P7QD', 'P7QE', 'P7QF', 'P7QG', 'P7QH', 'P7QI', 'P7QJ', 'P7QK', 'P7QL', 'P7QM', 'P7QN', 'P7QO', 'P7QP', 'P7QQ', 'P7QR', 'P7QS', 'P7QT', 'P7QU', 'P7QV', 'P7QW', 'P7QX', 'P7QY', 'P7QZ', 'P7RA', 'P7RB', 'P7RC', 'P7RD', 'P7RE', 'P7RF', 'P7RG', 'P7RH', 'P7RI', 'P7RJ', 'P7RK', 'P7RL', 'P7RM', 'P7RN', 'P7RO', 'P7RP', 'P7RQ', 'P7RR', 'P7RS', 'P7RT', 'P7RU', 'P7RV', 'P7RW', 'P7RX', 'P7RY', 'P7RZ', 'P7SA', 'P7SB', 'P7SC', 'P7SD', 'P7SE', 'P7SF', 'P7SG', 'P7SH', 'P7SI', 'P7SJ', 'P7SK', 'P7SL', 'P7SM', 'P7SN', 'P7SO', 'P7SP', 'P7SQ', 'P7SR', 'P7SS', 'P7ST', 'P7SU', 'P7SV', 'P7SW', 'P7SX', 'P7SY', 'P7SZ', 'P7TA', 'P7TB', 'P7TC', 'P7TD', 'P7TE', 'P7TF', 'P7TG', 'P7TH', 'P7TI', 'P7TJ', 'P7TK', 'P7TL', 'P7TM', 'P7TN', 'P7TO', 'P7TP', 'P7TQ', 'P7TR', 'P7TS', 'P7TT', 'P7TU', 'P7TV', 'P7TW', 'P7TX', 'P7TY', 'P7TZ', 'P7UA', 'P7UB', 'P7UC', 'P7UD', 'P7UE', 'P7UF', 'P7UG', 'P7UH', 'P7UI', 'P7UJ', 'P7UK', 'P7UL', 'P7UM', 'P7UN', 'P7UO', 'P7UP', 'P7UQ', 'P7UR', 'P7US', 'P7UT', 'P7UU', 'P7UV', 'P7UW', 'P7UX', 'P7UY', 'P7UZ', 'P7VA', 'P7VB', 'P7VC', 'P7VD', 'P7VE', 'P7VF', 'P7VG', 'P7VH', 'P7VI', 'P7VJ', 'P7VK', 'P7VL', 'P7VM', 'P7VN', 'P7VO', 'P7VP', 'P7VQ', 'P7VR', 'P7VS', 'P7VT', 'P7VU', 'P7VV', 'P7VW', 'P7VX', 'P7VY', 'P7VZ', 'P7WA', 'P7WB', 'P7WC', 'P7WD', 'P7WE', 'P7WF', 'P7WG', 'P7WH', 'P7WI', 'P7WJ', 'P7WK', 'P7WL', 'P7WM', 'P7WN', 'P7WO', 'P7WP', 'P7WQ', 'P7WR', 'P7WS', 'P7WT', 'P7WU', 'P7WV', 'P7WW', 'P7WX', 'P7WY', 'P7WZ', 'P7XA', 'P7XB', 'P7XC', 'P7XD', 'P7XE', 'P7XF', 'P7XG', 'P7XH', 'P7XI', 'P7XJ', 'P7XK', 'P7XL', 'P7XM', 'P7XN', 'P7XO', 'P7XP', 'P7XQ', 'P7XR', 'P7XS', 'P7XT', 'P7XU', 'P7XV', 'P7XW', 'P7XX', 'P7XY', 'P7XZ', 'P7YA', 'P7YB', 'P7YC', 'P7YD', 'P7YE', 'P7YF', 'P7YG', 'P7YH', 'P7YI', 'P7YJ', 'P7YK', 'P7YL', 'P7YM', 'P7YN', 'P7YO', 'P7YP', 'P7YQ', 'P7YR', 'P7YS', 'P7YT', 'P7YU', 'P7YV', 'P7YW', 'P7YX', 'P7YY', 'P7YZ', 'P7ZA', 'P7ZB', 'P7ZC', 'P7ZD', 'P7ZE', 'P7ZF', 'P7ZG', 'P7ZH', 'P7ZI', 'P7ZJ', 'P7ZK', 'P7ZL', 'P7ZM', 'P7ZN', 'P7ZO', 'P7ZP', 'P7ZQ', 'P7ZR', 'P7ZS', 'P7ZT', 'P7ZU', 'P7ZV', 'P7ZW', 'P7ZX', 'P7ZY', 'P7ZZ

References

1) Abdo, A. A. et al., The on-orbit calibration of the Fermi Large Area Telescope, *Astronomical Journal* 132 (2006).

2) Anderson, M. et al., The Fermi Large Area Telescope on-orbit Event Class System, *International Journal of Space and Astronautics* 10 (2007).

Bregnon

Pass 8

- Presented in detail in posters on **ACD pile-up correction, CAL reconstruction, track reconstruction, and event-level analysis, plus an overview**
- Pass 8 is built on a fundamental reimplementaion of the reconstruction

Pass 8: Toward the Full Realization of the Fermi LAT Scientific Potential

W. Atwood¹, L. Baldo², P. Bruel³, E. Charles⁴, and T. Usher¹
 on behalf of the Fermi Large Area Telescope Collaboration
¹Santa Cruz Institute for Particle Physics, University of California, Santa Cruz CA
²University of Pisa and INFN Pisa
³LLR, École polytechnique, IN2P3/CNRS
⁴SLAC National Accelerator Laboratory, Menlo Park CA

Summary: Overview and prospects for the Fermi LAT Pass 8 event level analysis.

The event selection developed for the Fermi Large Area Telescope before launch has been periodically updated to reflect the constantly improving knowledge of the detector and the environment in which it operates. Pass 7, released to the public in August 2011, represents the most recent major iteration of this incremental process. In parallel, the LAT team has undertaken a coherent long-term effort aimed at a radical revision of the entire event-level analysis, based on the experience gained in the first phase of the mission. This includes virtually every aspect of the data reduction process, from the simulation of the detector to the event reconstruction and the background rejection. The potential improvements include (and are not limited to): a significant reduction in background contamination coupled with an increased effective area, a better understanding of the systematic uncertainties and an extension of the energy reach for the photon analysis below 100 MeV and above 100 GeV. We present an overview of the work that has been done or is ongoing and the prospects for the near future.

Introduction

The current LAT event-level analysis was largely developed before launch using Monte Carlo simulations in a series of iterations that we call Passes. Pass 6 was released at launch and followed (in August 2011) by Pass 7, which mitigated the impact of some of the limitations of its predecessor. On-orbit experience with the fully imaged detector has revealed some neglected and overlooked issues—primarily (but not only) the effect of the instrumental pile-up (aka “Clear Events”). Clear improvements, with the potential to greatly extend the LAT science capabilities, have been identified at all the main steps:

- Monte Carlo simulation of the detector;
- Event reconstruction;
- Background rejection.

Tracker Reconstruction [see T. Usher, poster]

Current framework—track-by-track combinatorial pattern recognition

- Track confusion and errors in high-multiplicity events;
- Energy reach effectively limited by mistacking.

Pass 8—global line-based approach to track finding

- Reduce mistacking, improve the high-energy Point Spread Function (PSF);
- Provide additional information for the background rejection.

More development areas: Kalman fit measurement errors, PSF analysis, buffer truncation [see L. Rochester, poster], cosmic-ray tracking, ghost tracking, neural energy vetoing.

Calorimeter Reconstruction [see C. Sgró, poster]

Current framework—the calorimeter is treated as a monolithic whole.

- Background rejection—compromised by instrumental pile-up;
- No chance to see multi-photon events.

Pass 8—clustering stage added at the beginning of the reconstruction chain.

- Separate the pile-up activity from the genuine gamma-ray signal;
- Provide topology information to the following reconstruction steps.

More development areas: light collection simulation, position reconstruction, cluster classification, moments analysis and direction reconstruction, fiducial rejection, crystal saturation, energy reconstruction beyond 1 TeV [see P. Bruel, poster].

ACD Reconstruction [see A. D’Elia Wagner, poster]

Current framework—track/file association in physical distance.

- Explicit energy-dependent cuts;
- Susceptible to global pile-up at low energy.

Pass 8—track and cluster/file association based on covariant error propagation

- Improved background rejection;
- Use trigger veto to suppress pile-up.

Physics Potentials

Pass 8 will approach the full scientific potential of the LAT.

- Lower backgrounds and better control over the systematic uncertainties;
- Extension of the energy reach:
 - Below 100 MeV, improved energy resolution and background rejection (hadronic vs. leptonic emission);
 - Above 100 GeV, less tracking confusion, better compensation for calorimeter saturation (below γ and cosmic-ray γ $\rightarrow \pi^+ \pi^-$ spectra above 1 TeV).
- Better high-energy Point Spread Function (AGN per halo);
- Recover calorimeter-only events for science analysis (substantial effective area increase above 20 GeV);
- Multi-photon events (coherent γ -ray production in AGNs and GRBs);
- γ -ray polarimetry.

Ongoing Developments

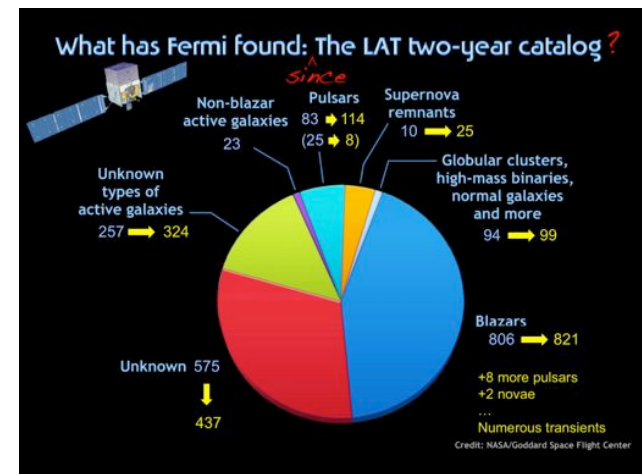
- Integrate reconstruction improvements into a coherent event structure;
- Beginning work on the background rejection [see M. Wood, poster]:
 - Start from the basic components of the Pass 7 analysis;
 - New, flexible analysis framework under development;
 - Define provisional event classes to start assessing the performance improvements.
- Definition of a set of key science projects:
 - Use small-size reprocessed flight data sets;
 - Benchmark the new event reconstruction on real science projects [see M. Pavesi-Rollin, poster].

The Authors wish to acknowledge the substantive and diverse contribution of the Pass 8 working group members. Many of the items briefly mentioned here are more thoroughly described in dedicated posters.

Atwood

News on New Catalogs

- Ferrara overview of follow-up work on classifying, associating, and identifying 2FGL sources and plans for a 5-year LAT catalog
- 1FHL: >10 GeV LAT sources (3 years, 514 sources, 63 are not 2FGL and many of interest to IACTs) (Paneque)
- FAVA: Systematic search for variability on weekly timescales, sensitive and diffuse emission model-free – apparently a Nova detector (Allafort)
- LAT GRBs: 35 GRBs (7 LLE-only) (Vianello)
- GBM catalogs: Time-resolved Spectral (bright burst) catalog was also mentioned by von Kienlin/Greiner



Ferrara



Lots more to do!

- Near-term upcoming results
 - Second LAT pulsar catalog [P. Ray, Monday]
 - Catalog of LAT-detected SNR [T. Brandt, Tuesday]
 - Catalog of LAT sources at >10 GeV [D. Paneque, next]
 - Catalog of Flaring LAT sources [A. Allafort, just after]
 - List of LAT-detected TGFs [J. Grove, Wednesday]
 - List of LAT-detected solar flares [N. Omodei, Monday]
 - Extension of both GBM GRB catalogs for years 3 & 4 [A. von Kienlin, after that]
 - Catalog of joint Fermi-Interplanetary Network GRBs
 - Update to GBM-detected TGFs [V. Connaughton, Monday]
 - Type-1 X-ray bursts in GBM
- 5-year catalog of LAT point sources

Multiwavelength Session

- Organized by Chuck Dermer & Liz Hays: Radio through TeV in wavelength order + GW
- Dave Thompson opened by urging coordinated MW campaigns
- **Radio telescope arrays** (Alexander van der Horst)
 - With an emphasis on LOFAR and correlative studies with GBM
- **Planck & WMAP** (Isabelle Grenier) microwave
 - Impact on diffuse emission studies, SNRs, AGNs
- **NuSTAR** (Greg Madejski) hard X-ray imaging
 - Joint monitoring campaigns with *Fermi* are being planned
- **aLIGO** (Lindy Blackburn for Cole Miller) gravitational wave
 - Sensitivity will soon reach the level at which NS-NS mergers (face on) should be detected at a few per year rate
 - Contemporaneous operation with GBM is important
- **HAWC** (Brenda Dingus) sky monitoring in the >1 TeV range
 - 30 tanks now, 100 next year, on the way to 300 “HAWC will observe Galactic GeV sources with the same significance as *Fermi*”
- **CTA** (David Williams) will begin construction in “~2015”
 - Will “build on the *Fermi* legacy”

Multimessenger Too

- Neutrino astronomy is being applied to follow up *Fermi* results

Neilson

ICECUBE NEUTRINO ANALYSES
MOTIVATED BY FERMI-LAT OBSERVATIONS

Naoko Kurahashi Neilson
For The IceCube Collaboration
naoko@icecube.wisc.edu
University of Wisconsin, Madison

The detector, data, and event selection
The IceCube neutrino observatory instruments a cubic kilometer of ice at the South Pole using 86 strings of optical sensors. The detector was built over several years and took data while construction progressed until completion in 2011. The analysis presented here uses two years of data, one year using the 40 string detector and another with the 86-string. Over 140,000 events were selected after cuts based on quality of reconstructed tracks to neutrino-induced muons, and estimated energy. At 10 TeV the median angular resolution is ~1° in the northern sky, the atmospheric neutrino background dominates making the full-Flavor region optimal for astrophysical source searches. In the southern hemisphere, high energy atmospheric neutrinos become the main background increasing the source sensitivity energy range to PeV-EeV.

Diffuse Neutrino Search from the Galactic Plane
Deciding where to look
The diffuse flux of neutrinos along the galactic plane is not expected to be uniform. A spatial template to test must be chosen. The question is then whether neutrino production in the plane traces high-energy cosmic ray source location (as shown to the right, or the matter (gas) density.

Likelihood Analysis
A likelihood analysis is performed using the expected neutrino annual distribution map, $S(\alpha, \delta)$ is the signal PDF which is the value at a taken from the spatial map multiplied by the energy PDF value taken from the distribution of energy seen in data at a given declination band. The binned spatial PDF is calculated using the number of observed events vs. $\alpha \cos \delta$.

Fermi Bubbles Search
Large bilateral bubbles reported in Fermi LAT data (Ding et al., 2013 (JUL 13)) have been suggested to be of hadronic origin (Crocker and Marazziti, 2011 (FEB 04); Liu, 1993). Neutrino emission would be evidence of pion decays occurring in these regions. We suggest an analysis to look for neutrinos from these bubbles.

Stacking Searches
Fermi Bright Source List with *Milagro* observations
Sources in Fermi's BSL with associated observations in the *Milagro* experiment (A. A. Abdo et al., 2009 (JUL 10)) are selected along with sources of high or intermediate flux or observation in *Milagro* to define a stacking sample.

ON/OFF zones approach
ON/OFF zones approach
ON/OFF zones approach
ON/OFF zones approach

Data/MC comparison
Data/MC comparison
Data/MC comparison
Data/MC comparison

Unblinding and results
Unblinding and results
Unblinding and results
Unblinding and results

Biagi

Search for Neutrino Emission from the Fermi Bubbles with the ANTARES Telescope

Simone Biagi
University of Bologna and INFN
on behalf of the ANTARES Collaboration

The search for neutrinos from the Fermi Bubbles (FB) using ANTARES has been completed in the period 2007-2010. It is presented here the results of the search for neutrinos from the Fermi Bubbles. The Fermi Bubbles are extended regions that cover ~18° in the sky, centered around the Galactic Center and extend approximately 50 kpc in the Galactic Plane (Fig. 1). The bubbles are characterized by gamma emission with a spectrum ~100 GeV with a relatively constant intensity all over the region (2). According to a standard neutrino production mechanism for gamma emission (3), the Fermi Bubbles can be a source of high-energy neutrinos. From the measured gamma flux, it is possible to derive the neutrino flux (4).

Neutrino flux = $0.4 \text{ GeV/cm}^2/\text{sr/yr}$
Energy index = $1.00 \text{ GeV/cm}^2/\text{sr/yr}$

1. The ANTARES neutrino telescope
The ANTARES neutrino telescope is located in the Mediterranean Sea, 400 km off the coast of Corsica. It is composed of 24.62 strings of 308 optical modules arranged in 12 strings (Fig. 2). The main scientific goal is the search for cosmic neutrinos coming from galactic and extragalactic sources. Neutrinos are detected through the Cherenkov light emitted along the path of charged particles produced in neutrino interaction inside or in the vicinity of the detector. ANTARES is sensitive to all flavor neutrinos. It is approved for these neutrinos.

2. ON/OFF zones approach
The ON/OFF zones approach is used to search for neutrinos from the Fermi Bubbles. The ON/OFF zones approach is used to search for neutrinos from the Fermi Bubbles. The ON/OFF zones approach is used to search for neutrinos from the Fermi Bubbles.

3. Data/MC comparison
The data/MC comparison is used to search for neutrinos from the Fermi Bubbles. The data/MC comparison is used to search for neutrinos from the Fermi Bubbles. The data/MC comparison is used to search for neutrinos from the Fermi Bubbles.

4. Unblinding and results
The unblinding and results are used to search for neutrinos from the Fermi Bubbles. The unblinding and results are used to search for neutrinos from the Fermi Bubbles. The unblinding and results are used to search for neutrinos from the Fermi Bubbles.

Outlook

A Broader Perspective

- Roger Blandford on “what will you have done for us lately?” described Fermi science in context of 5 broader topics in astrophysics, pointing out that discovery and understanding are more fun than upper limits
- **Dark matter** – 23% of contemporary universe
 - 30 direct detection experiments and they need to get bigger
 - Indirect detection (gamma rays, positrons) has astrophysical uncertainties
- **Black holes** from GRB scale (formation) to AGNs*
- **Detection of gravitational radiation** – Fermi can help it become astronomy
- **Extreme electrodynamics** – EA currents and PV voltages
- “I believe that the best is yet to come from Fermi and that is not belittling the considerable accomplishments that have come before.”

Outlook: A Fermi Science Metric

- As an O *Fermi* h the exp field and of the s from ga astrono *Compton Gamma Ray Observatory* fostered
- Julie illustrated this with a chart of GI proposal submission counts

The 2013 Fermi Summer School will take place in Lewes, Delaware, May 27-June 5, 2013. Sponsored by the mission it is a great way to get up to speed on Fermi science and analysis.



* From http://fermi.gsfc.nasa.gov/cgi-bin/bibliography_fermi selecting all publications that present analysis of Fermi data and/or refer to published Fermi results and/or predict Fermi results

Outlook: Looking Back

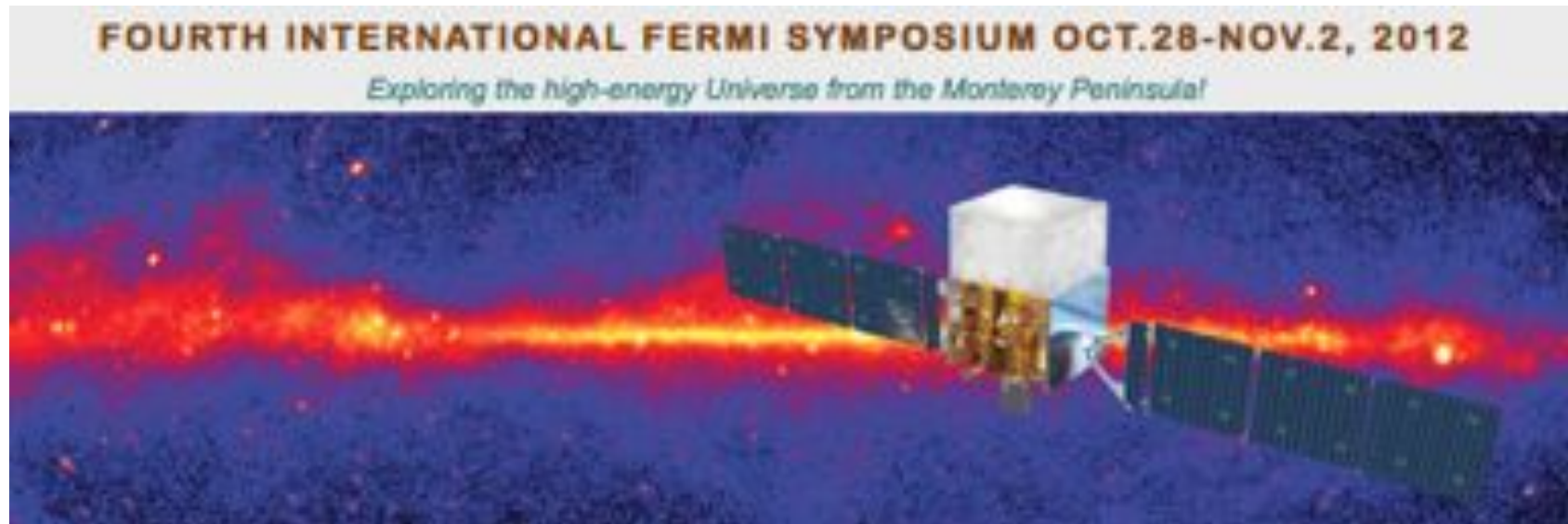
- Don Kniffen reminded us that the scientific drivers for the balloon and then satellite experiments in high-energy gamma-ray astronomy usually have **not** turned out to be the big discovery or selling point for the **next** experiment. Timeline:

Optimistic predictions -> Balloon experiments -> Better balloon experiments -> [Evidence for diffuse flux] -> SAS-2/COS-B -> [Diffuse flux and pulsars] -> EGRET -> [Blazars] -> AGILE, Fermi ->

Current Outlook

- For **Fermi**: good if you keep making discoveries, writing papers, and finding the ‘science drivers’
- For high-energy gamma-ray astronomy more broadly: also good
 - Ground-based: **H.E.S.S. (I.I.)**, **MAGIC**, and **VERITAS** have all recently completed upgrades and big advances are coming from **HAWC** and **CTA**
 - **AGILE** is still flying and **Gamma-400** has promise as the next space mission in the GeV range

Thank You



Highlights from the 5th Fermi Symposium

- Pass 8 in wide use
- 3FGL